

{NASA-TM-84245) AN EXPERIMENTAL STUDY OF  
DYNAMIC STALL ON ADVANCED AIRFOIL SECTIONS.  
VOLUME 3: HOT-WIRE AND HOT FILM  
MEASUREMENTS (NASA) 69 p HC A04/MF A01

83-17505

Unclass  
CSCL 01A 33/02 02717

---

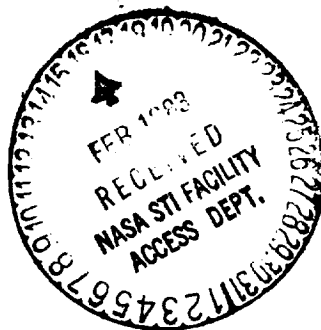
# An Experimental Study of Dynamic Stall on Advanced Airfoil Sections Volume 3. Hot-Wire and Hot-Film Measurements

---

L. W. Carr, W. J. McCroskey, K. W. McAlister,  
S. L. Pucci, and O. Lambert

---

December 1982



**NASA**  
National Aeronautics and  
Space Administration

REPRODUCED BY  
U.S. DEPARTMENT OF COMMERCE  
NATIONAL TECHNICAL  
INFORMATION SERVICE  
SPRINGFIELD, VA 22161

United States Army  
Aviation Research  
and Development  
Command





---

# **An Experimental Study of Dynamic Stall on Advanced Airfoil Sections Volume 3. Hot-Wire and Hot-Film Measurements**

---

L. W. Carr

W. J. McCroskey

K. W. McAlister

S. L. Pucci, Aeromechanics Laboratory

AVRADCOM Research and Technology Laboratories

Ames Research Center, Moffett Field, California

O. Lambert, Service Technique des Constructions Aeronautiques,

Paris, France

**NASA**

National Aeronautics and  
Space Administration

**Ames Research Center**  
Moffett Field, California 94035

United States Army  
Aviation Research and  
Development Command  
St. Louis, Missouri 63166





TABLE OF CONTENTS

	<u>Page</u>
LIST OF FIGURES . . . . .	v
LIST OF TABLES . . . . .	ix
SYMBOLS . . . . .	xi
SUMMARY . . . . .	1
INTRODUCTION . . . . .	1
DESCRIPTION OF EXPERIMENTAL PROCEDURES . . . . .	1
DATA ANALYSIS AND INTERPRETATION . . . . .	2
Skin-Friction Gage . . . . .	2
Hot-Wire Probe . . . . .	3
Reverse-Flow Sensors . . . . .	3
Averaging Techniques . . . . .	4
Example of Signal Analysis . . . . .	4
RESULTS . . . . .	4
REFERENCES . . . . .	6
TABLES . . . . .	7
FIGURES . . . . .	36

**PRECEDING PAGE BLANK NOT FILMED**



LIST OF FIGURES

	<u>Page</u>
1 Diagram showing installation of spar and airfoil shell in tunnel . . . . .	36
2 Diagram of hot-film skin-friction gage . . . . .	37
3 Response of hot-film skin-friction gages mounted on Ames A-01 airfoil during airfoil oscillation in pitch ( $\alpha = 15^\circ + 10^\circ \sin \omega t$ , $k = 0.10$ , $M_\infty = 0.22$ ) . . . . .	37
4 Response of hot-film skin-friction gages at surface of NACA 0012 airfoil during airfoil oscillation in pitch ( $\alpha = 15^\circ + 10^\circ \sin \omega t$ , $k = 0.10$ , $M_\infty = 0.295$ ) . . . . .	38
5 Diagram of dual-element hot-wire probe . . . . .	38
6 Response of hot-wire anemometer probes on Wortmann FX-098 airfoil during airfoil oscillation in pitch ( $\alpha = 15^\circ + 10^\circ \sin \omega t$ , $k = 0.10$ , $M_\infty = 0.11$ ) . . . . .	39
7 Response of hot-wire anemometer probe installed near trailing edge of the Vertol VR-7 airfoil during oscillation in pitch . . . . .	39
8 Results obtained using triple-wire flow-reversal sensor: (a) Typical comparison of flow-reversal sensor and hot-wire anemometer signal (from ref. 2); (b) Progression of flow reversal up airfoil during dynamic stall (from ref. 2) . . . . .	40
9 Diagram of three-element, directionally sensitive hot-wire probe (from ref. 2) . . . . .	41
10 Comparison of 100-cycle ensemble average and single-cycle signals from hot-wire anemometers for Vertol VR-7 airfoil during oscillation in pitch: ———, 100 cycle average; -----, single cycle . . . . .	42
11 Response of hot-film skin-friction gage and hot-wire anemometer probes on Vertol VR-7 during oscillation in pitch ( $\alpha = 15^\circ + 10^\circ \sin \omega t$ , $k = 0.10$ , $M_\infty = 0.185$ ) . . . . .	43
12 Phase angle, $\omega t$ , of flow reversal on NACA 0012 airfoil vs chord location for a range of Mach numbers at $k = 0.1$ , $\alpha = 15^\circ + 10^\circ \sin \omega t$ - Mach number effects . . . . .	44
13 Phase angle, $\omega t$ , of flow reversal on Ames A-01 airfoil vs chord location for a range of Mach numbers at $k = 0.1$ , $\alpha = 15^\circ + 10^\circ \sin \omega t$ - Mach number effects . . . . .	45
14 Phase angle, $\omega t$ , of flow reversal on Wortmann FX-098 airfoil vs chord location for a range of Mach numbers at $k = 0.1$ , $\alpha = 15^\circ + 10^\circ \sin \omega t$ - Mach number effects . . . . .	46

PRECEDING PAGE BLANK NOT FILMED

15	Phase angle, $\omega t$ , of flow reversal on Sikorsky SC-1095 airfoil vs chord location for a range of Mach numbers at $k = 0.1$ , $\alpha = 15^\circ + 10^\circ \sin \omega t$ - Mach number effects . . . . .	47
16	Phase angle, $\omega t$ , of flow reversal on Hughes HH-02 airfoil vs chord location for a range of Mach numbers at $k = 0.1$ , $\alpha = 15^\circ + 10^\circ \sin \omega t$ - Mach number effects . . . . .	48
17	Phase angle, $\omega t$ , of flow reversal on Vertol VR-7 airfoil vs chord location for a range of Mach numbers at $k = 0.1$ , $\alpha = 15^\circ + 10^\circ \sin \omega t$ - Mach number effects . . . . .	49
18	Phase angle, $\omega t$ , of flow reversal on NLR-1 airfoil vs chord location for a range of Mach numbers at $k = 0.1$ , $\alpha = 15^\circ + 10^\circ \sin \omega t$ - Mach number effects . . . . .	50
19	Phase angle, $\omega t$ , of flow reversal on NLR-7 airfoil vs chord location for a range of Mach numbers at $k = 0.1$ , $\alpha = 15^\circ + 10^\circ \sin \omega t$ - Mach number effects . . . . .	51
20	Phase angle, $\omega t$ , of flow reversal on NACA 0012 airfoil vs chord location for a range of frequencies at $M_\infty = 0.295$ , $\alpha = 12^\circ + 5^\circ \sin \omega t$ - light-stall conditions . . . . .	51
21	Phase angle, $\omega t$ , of flow reversal on Ames A-01 airfoil vs chord location for a range of frequencies at $M_\infty = 0.295$ , $\alpha = 11^\circ + 5^\circ \sin \omega t$ - light-stall conditions . . . . .	52
22	Phase angle, $\omega t$ , of flow reversal on Wortmann FX-098 airfoil vs chord location for a range of frequencies at $M_\infty = 0.295$ , $\alpha = 10^\circ + 5^\circ \sin \omega t$ - light-stall conditions . . . . .	52
23	Phase angle, $\omega t$ , of flow reversal on Sikorsky SC-1095 airfoil vs chord location for a range of frequencies at $M_\infty = 0.295$ , $\alpha = 11^\circ + 5^\circ \sin \omega t$ - light-stall conditions . . . . .	53
24	Phase angle, $\omega t$ , of flow reversal on Hughes HH-02 airfoil vs chord location for a range of frequencies at $M_\infty = 0.295$ , $\alpha = 10^\circ + 5^\circ \sin \omega t$ - light-stall conditions . . . . .	53
25	Phase angle, $\omega t$ , of flow reversal on Vertol VR-7 airfoil vs chord location for a range of frequencies at $M_\infty = 0.295$ , $\alpha = 15^\circ + 5^\circ \sin \omega t$ - light-stall conditions . . . . .	54
26	Phase angle, $\omega t$ , of flow reversal on NLR-1 airfoil vs chord location for a range of frequencies at $M_\infty = 0.295$ , $\alpha = 10^\circ + 5^\circ \sin \omega t$ - light-stall conditions . . . . .	54
27	Phase angle, $\omega t$ , of flow reversal on NLR-7 airfoil vs chord location for a range of frequencies at $M_\infty = 0.295$ , $\alpha = 15^\circ + 5^\circ \sin \omega t$ - light-stall conditions . . . . .	55



	<u>Page</u>
28 Phase angle, $\omega t$ , of flow reversal on Ames A-01 airfoil vs chord for a range of frequencies at $M_\infty = 0.295$ , $\alpha = 15^\circ + 10^\circ \sin \omega t$ - deep-stall conditions . . . . .	56
29 Phase angle, $\omega t$ , of flow reversal on Wortmann W-98 airfoil vs chord for a range of frequencies at $M_\infty = 0.295$ , $\alpha = 15^\circ + 10^\circ \sin \omega t$ - deep-stall conditions . . . . .	57
30 Phase angle, $\omega t$ , of flow reversal on Wortmann FX-098 airfoil vs chord for a range of frequencies at $M_\infty = 0.185$ , $\alpha = 15^\circ + 10^\circ \sin \omega t$ - deep-stall conditions . . . . .	58
31 Phase angle, $\omega t$ , of flow reversal on Vertol VR-7 airfoil vs chord for a range of frequencies at $M_\infty = 0.295$ , $\alpha = 15^\circ + 10^\circ \sin \omega t$ - deep-stall conditions . . . . .	59



LIST OF TABLES

	<u>Page</u>
1 Summary of analyzed flow-reversal data . . . . .	7
2 Phase angle of flow reversal: NACA 0012 airfoil . . . . .	7
3 Phase angle of flow reversal: Ames A-01 airfoil . . . . .	8
4 Phase angle of flow reversal: Wortmann FX-098 airfoil . . . . .	9
5 Phase angle of flow reversal: Sikorsky SC-1 airfoil . . . . .	10
6 Phase angle of flow reversal: Hughes HH-02 airfoil . . . . .	10
7 Phase angle of flow reversal: Vertol VR-7 airfoil . . . . .	11
8 Phase angle of flow reversal: NLR NL-1 airfoil . . . . .	12
9 Phase angle of flow reversal: NLR-7301 airfoil . . . . .	12
10 Error-bound for flow-reversal measurements (deg): NACA 0012 airfoil . . . . .	13
11 Error-bound for flow-reversal measurements (deg): Ames A-01 airfoil . . . . .	14
12 Error-bound for flow-reversal measurements (deg): Wortmann FX-098 airfoil . . . . .	15
13 Error-bound for flow-reversal measurements (deg): Hughes HH-02 airfoil . . . . .	16
14 Error-bound for flow-reversal measurements (deg): Vertol VR-7 airfoil . . . . .	17
15 Error-bound for flow-reversal measurements (deg): NLR-1 airfoil . . . . .	18
16 Error-bound for flow-reversal measurements (deg): NLR-7301 airfoil . . . . .	18
17 Notes pertaining to tables 18 to 25 . . . . .	19
18 Catalog of recorded data: NACA 0012 airfoil . . . . .	20
19 Catalog of recorded data: Ames A-01 airfoil . . . . .	22
20 Catalog of recorded data: Wortmann FX-098 airfoil . . . . .	24
21 Catalog of recorded data: Sikorsky SC-1095 airfoil . . . . .	26
22 Catalog of recorded data: Hughes HH-02 airfoil . . . . .	28

	<u>Page</u>
23 Catalog of recorded data: Vertol VR-7 airfoil . . . . .	30
24 Catalog of recorded data: NLR-1 airfoil . . . . .	32
25 Catalog of recorded data: NLR-7301 airfoil . . . . .	34

## SYMBOLS

C	chord, m
CM	moment coefficient
CN	normal force coefficient
FR	flow reversal
HF	hot-film
HW	hot-wire
k	reduced frequency
LS	lift stall
M	free-stream Mach number
MS	moment stall
NFR	no flow reversal detected
R	reattachment
T1	transition from turbulent to laminar flow
T2	transition from laminar to turbulent flow
t	time, sec
u	local velocity, m/sec
x	distance along the chord, m
$\alpha$	angle of incidence, deg
$\omega$	rotational frequency, rad/sec



# AN EXPERIMENTAL STUDY OF DYNAMIC STALL ON ADVANCED AIRFOIL SECTIONS

## VOLUME 3. HOT-WIRE AND HOT-FILM MEASUREMENTS

L. W. Carr, W. J. McCroskey, K. W. McAlister, and S. L. Pucci

U.S. Army Aeromechanics Laboratory (AVRADCOM), Ames Research Center

and

O. Lambert

Service Technique des Constructions Aeronautiques, Paris, France

### SUMMARY

Detailed unsteady boundary-layer measurements are presented for eight airfoils oscillated in pitch through the dynamic-stall regime. The present report (the third of three volumes) describes the techniques developed for analysis and evaluation of the hot-film and hot-wire signals, offers some interpretation of the results, and tabulates all the cases in which flow reversal has been recorded.

### INTRODUCTION

The study of dynamic stall of oscillating airfoils has demonstrated the need for obtaining detailed boundary-layer data during the stall process. Results from the present experiment show that boundary-layer characteristics can be significantly altered by airfoil shape, and that the boundary-layer behavior is sensitive to many parameters associated with the airfoil motion. These conclusions are based on analysis of signals from hot-wire and hot-film probes mounted near or at the surface of the various airfoils. However, evaluation of hot-wire data is very subjective, and presents a formidable analytical task. The present report describes the techniques developed for analysis and evaluation of the hot-film and hot-wire signals, offers some interpretations of the results, and tabulates all the cases in which flow-reversal data have been recorded. An overview of the experiment has been presented in reference 1; a detailed summary of this test and the experimental conditions that were studied is presented in volume 1 of the present report; details of the pressure distribution results, along with lift and moment data are presented in volume 2. The present report presents the corresponding details of the viscous flow measurements that were obtained.

### DESCRIPTION OF EXPERIMENTAL PROCEDURES

The experiment was designed to allow accurate testing of various airfoils under virtually identical operating conditions. Therefore each airfoil profile was machined into a shell which could be attached to the metal spar that contained all the instrumentation. After each airfoil profile was tested, the instrumentation was removed from the shell; it then remained with the spar, ready for installation of the next shell. In this way, the various profiles could be tested using identical

instrumentation and oscillation mechanisms; details of this system are presented in reference 1; figure 1 is a diagram of the spar with a shell installed. Instantaneous single-surface pressure measurements were obtained for a wide range of test conditions. Hot-wire, hot-film measurements, or both, were made near the airfoil surface to determine the flow-reversal characteristics for each test condition. Three different types of hot-wire anemometer sensors were used during the oscillating airfoil test: hot-film surface skin-friction gages, dual hot-wire probes, and triple-wire flow-reversal sensors. The most common configurations had either six hot-films along the airfoil upper surface, or one hot-film at the leading edge ( $x/C = 0.025$ ) and five hot-wires distributed along the upper surface. The data were recorded on 32-channel analog tape, with a timing code that allowed comparison of hot-wire data and the pressure data, which were recorded separately for each test condition.

## DATA ANALYSIS AND INTERPRETATION

### Skin-Friction Gage

The skin-friction gage that was used during a major portion of the test program consisted of an alumina-coated platinum surface element epoxied into a metal sleeve (see fig. 2). This sensor, which was very resistant to damage, was used for much of the oscillating airfoil test program. However, the characteristics of this probe design must be taken into account when analyzing the output signals.

The output from the hot-film probe is related to the shear stress; when flow reversal occurs, the instantaneous value of shear stress passes through zero, and there is a local minimum in the resultant signal. Unfortunately, a significant part of the energy supplied to the probe element is transmitted from the element to the substrate of the gage. This heat transfer results in a relatively high dc-offset in the output voltage of the probe. In addition, this heat transfer causes the minimum value of the hot-film signal to decrease slowly with time, even when the flow is fully separated (with a nominal shear-stress value = 0). These effects can make the interpretation of the signal somewhat difficult.

Figure 3 presents an example of the output from skin-friction gages mounted near the leading edge of the Ames A-01 airfoil during oscillation. At the marker "T1," the flow has passed through transition from turbulent to laminar flow, with a resultant reduction in shear stress and decrease in fluctuation intensity. The flow remains laminar during the low-angle portion of the cycle; as the angle increases, transition to turbulent flow occurs (at "T2"), and the skin-friction gage shows a corresponding increase in signal magnitude, as well as an increase in fluctuation amplitude. The next major event, marked by "FR," is the occurrence of flow reversal; this results in a drop in the magnitude of the shear stress. Note that the signal does not remain constant, even though the airfoil flow has separated; this continuing decrease is associated with the heat-transfer effects outlined earlier. Finally, marker "R" indicates the point when flow reattaches to the airfoil (during the down-stroke), beginning the oscillation cycle once more.

Unfortunately, the relatively crisp delineation of flow conditions that appears in figure 3 is not always present. Figure 4 shows an example of a less clear case of leading-edge flow: here, the development of flow reversal is relatively slow, and the decreasing of the signal to its minimum is difficult to separate from the decreasing of the minimum itself. The estimated flow-reversal points are marked by "FR."



## Hot-Wire Probe

Hot-wire anemometer measurements were performed using a dual-wire probe (see fig. 5); this dual-wire approach was chosen to reduce the chance of interruption of the test as a result of wire breakage; since both wires were being recorded, the loss of either wire would not mean the loss of flow-reversal information at that x-station. The output signal from a hot-wire probe is a nonlinear function of the local velocity; therefore, the signals were linearized and scaled such that the resultant signal was approximately proportional to the associated velocity. Figure 6 shows a representative example of hot-wire data for flow near the leading edge of the FX-098 airfoil.

As the angle of attack increases, transition to turbulent flow occurs at  $x/C = 0.025$ ; this is observed at "T2" in figure 6 for hot-wire probe HW1. Note that there is no dramatic change in the output signal magnitude. Transition on airfoils occurs at low angles of attack, for conditions where the boundary layer is thin. In these conditions, the hot-wire probe is often near or at the edge of the boundary layer. Therefore, the change of the velocity profile during transition has little or no effect on the value of  $U$ ; transition will mainly be marked by changes in the fluctuation level. The next major flow phenomenon is marked by "FR"; at this point the flow has separated from the airfoil, causing an abrupt decrease in the local velocity. Note that the hot-wire signal changes abruptly to zero, and then continues at a well-defined constant value (compare with the hot-film output of fig. 3). Later, reattachment occurs (at "R"); as the minimum angle is approached, the flow becomes laminar again, and the cycle repeats.

As was noted for the hot-film, the hot-wire results are not always clearly delineated. Figure 7 shows a hot-wire signal measured near the trailing edge of the VR-7 airfoil which was difficult to evaluate. The turbulence level in this signal is very high, and is masking the development of the periodic component of the signal. Because this turbulent component is superimposed on the periodic part of the signal, the instantaneous value of the signal reaches zero long before and after flow reversal of the ensemble-averaged flow (marked as "FR" in the figure) would have occurred. Therefore, the error band for signals measured near the trailing edge is significantly larger than those associated with leading-edge, or midchord locations.

## Reverse-Flow Sensors

A specially designed hot-wire probe was developed for evaluation of the flow reversal on the VR-7 airfoil. This airfoil has trailing-edge flow reversal during almost all unsteady flow conditions, and a better method was needed for determining the reversal point under these conditions. The probe is described in detail in reference 2; operation is based on the use of a highly heated center wire, with two additional wires, one upstream and one downstream of this heater, operated at low overheat ratio. These additional wires detect the heated wake of the center wire, and a comparison circuit is used to determine the instantaneous flow direction. This probe system can detect both the magnitude and the direction of the local flow, and is especially effective in regions of high-turbulence, low-velocity flow. Examples of the output from this probe are presented in figure 8; a diagram of the probe is presented in figure 9.

## Averaging Techniques

Ensemble-averaging is often used to extract determinate signals from unsteady turbulent flow data, and this approach was applied to the present hot-wire data. Figure 10 presents the results of an ensemble-average of 100 cycles of the hot-wire signals on the VR-7 airfoil. It is evident in this figure that cyclic averaging smears the flow-reversal signal (to the point where no approach to zero voltage is observable in the averaged signal). In contrast, note the data for the last cycle digitized (shown as dotted in fig. 10). In this case, there are several instances of zero velocity; there are also indications of vortex motion on the airfoil (in the 40, 60, and 80 percent  $x/C$  wire outputs), which cannot be observed in the averaged data. There were small but significant variations in the angle at which flow reversal occurred between one cycle and the next; therefore, averages based on mechanical timing marks were not always able to capture the flow phenomena. In fact, this variation was sufficient in the present case to completely obscure the flow-reversal point in the data (in order to properly correlate these data, a true conditional ensemble-averaging technique would be needed, possibly triggered by a change in the character of the leading-edge pressure). Therefore, although some of the hot-wire and hot-film data were digitized and cyclically averaged, the analysis presented in this report has been based on visual evaluation of the analog signals for each of several cycles, after which the values of  $\omega t$  associated with flow reversal for a given sensor were averaged.

### Example of Signal Analysis

Figure 11 shows an example of a set of hot-wire and hot-film analog signals obtained during one period of oscillation. The first three signals are the angle of attack, the lift coefficient, and the moment coefficient, showing the lift stall (LS) and the moment stall (MS). The next six signals come from anemometer sensors: one hot-film near the leading edge (HF1), and five hot-wire probes (HW1 to HW6). The markers on these signals refer to the various events that have an effect on the hot-wire and hot-film readings: FR - initiation of reversed flow; R - reattachment of flow; T1 - transition from turbulent to laminar flow; T2 - transition from laminar to turbulent flow (as determined from hot-film signals).

## RESULTS

Results similar to these have been analyzed for all eight airfoils. In particular, the phase angle  $\omega t$ , at which flow reversal first appears at the  $x/C$  location of each hot-wire or hot-film probe, has been documented for a range of Mach numbers, frequencies, and stall severity for each airfoil. These phase angles, determined by the techniques outlined earlier, have been recorded in degrees measured through the oscillation cycle, referenced to the mean angle, for  $d\alpha/dt > 0$ . Table 1 presents a summary of the analyzed flow-reversal data. The Mach number studies were performed for  $\alpha = 15^\circ + 10^\circ \sin \omega t$ ,  $k = 0.1$ , and cover Mach number conditions that range from incompressible values ( $M_\infty = 0.035$ ) to ones that include small regions of supersonic flow near the leading edge ( $M_\infty = 0.30$ ). The "light-stall" frequency studies present data for a range of frequencies at  $M = 0.30$ , where the amplitude and mean angle have been chosen to cause a slight overshoot of the static stall angle associated with each airfoil during the oscillatory motion. The "deep-stall" study presents data for a range of frequencies at  $M_\infty = 0.30$ ,  $\alpha = 15^\circ + 10^\circ \sin \omega t$  (deep stall has been defined in ref. 1 as a condition in which a fully developed vortex is formed during

the oscillation cycle). The experimental data in deep stall were less amenable to analysis — the results were more subjective and in some cases inconclusive. Therefore, the results for only three airfoils are reported.

The results of these surveys are presented graphically in figures 12 to 31. Figures 12 to 19 present Mach number effects for deep-stall conditions; figures 20 to 27 present frequency effects for light-stall conditions; and figures 28 to 31 present frequency effects for deep-stall conditions. These data are also presented in tabular form in tables 2 to 9. The error bounds for these surveys are presented in tables 10 to 16. Finally, a catalog of all the hot-film and hot-wire data that were recorded is presented in tables 17 to 25, tabulated according to the corresponding pressure data (stored in digital form, as explained in vols. 1 and 2).

## REFERENCES

1. McCroskey, W. J.; McAlister, K. W.; Carr, L. W.; Pucci, S. L.; Lambert, O.; and Indergand, R. F.: "Dynamic Stall on Advanced Airfoil Sections," J. of the American Helicopter Society, July 1981.
2. Carr, L. W.; and McCroskey, W. J.: "A Directionally Sensitive Hot-Wire Probe for Detection of Flow Reversal in Highly Unsteady Flows," in International Congress on Instrumentation in Aerospace Facilities 1979 Record, Sept. 1979, pp. 154-162.

TABLE 1.- SUMMARY OF ANALYZED FLOW-REVERSAL DATA

Airfoil	Mach No. <sup>a</sup>	Light stall <sup>c</sup>	Deep stall <sup>b</sup>
NACA 0012.	Film <sup>d</sup>	Film <sup>d</sup>	Comb. <sup>e</sup> Wire <sup>g</sup>
A-01	Film <sup>d</sup>	Film <sup>d</sup>	
FX-098	Wire <sup>g</sup>	Comb. <sup>e</sup>	
SC-1095	Film <sup>d</sup>	Film <sup>d</sup>	Comb. <sup>f</sup>
HH-02	Film <sup>d</sup>	Comb. <sup>e</sup>	
VR-7	Comb. <sup>e</sup>	Comb. <sup>e</sup>	
NLR-1	Film <sup>d</sup>	Film <sup>d</sup>	
NLR-7301	Film <sup>d</sup>	Film <sup>d</sup>	

<sup>a</sup>Mach number sweep  $\alpha = 15^\circ + 10^\circ \sin \omega t$ ,  $k = 0.1$ .

<sup>b</sup>Frequency sweep,  $\alpha = 15^\circ + 10^\circ \sin \omega t$ ,  $M = 0.295$ .

<sup>c</sup>Frequency sweep,  $\alpha = \alpha_0 + \alpha_1 \sin \omega t$ ,  $M = 0.29$ .

<sup>d</sup>Hot-film shear-stress gage.

<sup>e</sup>Hot film at  $x/c = 0.025$ ; hot wire at all other locations.

<sup>f</sup>Hot wire at 0.025, 0.10, 0.25; reverse-flow sensors at  $x/c = 0.4, 0.6, 0.8$

<sup>g</sup>Hot-wire velocity probe.

TABLE 2.- PHASE ANGLE OF FLOW REVERSAL: NACA 0012 AIRFOIL

Mach No.	x/c						Ref. frame
	0.025	0.100	0.250	0.400	0.600	0.800	
$\alpha = 15^\circ + 10^\circ \sin \omega t$ , $k = 0.1$							
0.036	10.0	0.0	1.0	3.0	6.0	12.5	8013
.076	50.0	46.5	40.0	35.5	23.0	15.0	8115
.110	59.5	54.5	44.5	40.0	35.5	19.5	2320
.145	67.0	61.5	50.5	50.5	47.0	35.0	2314
.185	60.5	53.0	45.0	41.5	36.5	30.0	2310
.220	43.5	39.0	38.0	36.5	35.5	27.5	2208
.250	21.5	24.5	26.0	29.0	29.5	33.5	2204
.270	14.5	16.5	18.0	21.0	28.0	28.5	2202
.280	10.5	15.0	21.0	21.5	23.0	24.0	2200
.290	8.0	13.0	16.0	20.5	24.0	20.5	2103
.295	8.5	10.5	13.5	16.5	22.0	20.5	2101
Reduced freq.	x/c						Ref. frame
	0.025	0.100	0.250	0.400	0.600	0.800	
$\alpha = 12^\circ + 5^\circ \sin \omega t$ , $M = 0.295$							
0.025	NFR	55.5	48.0	37.0	32.5	26.5	7201
.050	NFR	32.5	37.0	38.0	33.0	31.0	7204
.100	NFR	34.0	42.5	45.0	47.5	41.0	7206
.200	35.5	44.0	54.0	59.0	64.0	71.0	7208

ORIGINAL PAGE IS  
OF POOR QUALITY

TABLE 3.- PHASE ANGLE OF FLOW REVERSAL: Ames A-01 AIRFOIL

Mach No.	x/c						Ref. frame
	0.025	0.100	0.250	0.400	0.600	0.800	
$\alpha = 15^\circ + 10^\circ \sin \omega t, k = 0.1$							
0.076	48.5	48.5	32.5	26.5	25.5	22.5	24400
.110	56.5	47.5	35.5	33.5	37.5	43.5	24316
.185	56.5	53.0	31.5	34.0	38.0	44.5	24219
.220	53.5	46.5	32.5	33.0	39.0	28.5	24210
.250	29.5	29.0	26.0	29.5	32.0	33.5	24202
.280	18.0	19.5	19.5	23.0	27.0	31.5	24118
.295	12.0	16.0	17.5	19.5	23.0	28.5	24108
Reduced freq.	x/c						Ref. frame
	0.025	0.100	0.250	0.400	0.600	0.800	
$\alpha = 11^\circ + 5^\circ \sin \omega t, M = 0.295$							
0.010	NFR	63.5	59.5	59.5	59.0	55.5	30202
.050	NFR	96.0	72.0	68.5	65.5	56.5	25215
.010	Data too irregular to be analyzed						25217
$\alpha = 15^\circ + 10^\circ \sin \omega t, M = 0.295$							
0.010	NFR	12.0	6.5	5.0	5.0	2.0	30021
.025	12.5	15.5	11.5	11.0	11.0	11.0	31016
.05	12.0	16.0	12.0	14.5	18.5	24.5	31018
.100	14.5	17.5	17.5	19.0	27.5	31.0	31019
.150	23.0	28.5	23.5	28.0	33.5	38.5	31020

**ORIGINAL PAGE IS  
OF POOR QUALITY**

**TABLE 4.- PHASE ANGLE OF FLOW REVERSAL: Wortmann FX-098 AIRFOIL**

Mach No.	x/c						Ref. frame
	0.025	0.100	0.250	0.400	0.600	0.800	
$\alpha = 15^\circ + 10^\circ \sin \omega t, k = 0.1$							
0.036	2.5	-1.2	-3.6	-2.0	-4.6	-8.6	16022
.076	36.5	34.5	27.0	18.5	14.5	4.5	16106
.110	43.0	39.5	32.5	24.5	16.5	10.5	16115
.185	37.0	37.0	36.5	33.5	31.0	24.0	16201
.220	22.5	24.5	25.0	26.5	24.0	21.5	16301
.250	14.5	15.5	18.0	18.0	17.5	21.5	16309
.280	9.0	12.0	18.0	20.0	17.5	15.5	22209
.295	6.5	12.5	15.5	16.5	18.5	21.0	22202
Reduced freq.	x/c						Ref. frame
	0.25	0.100	0.250	0.400	0.600	0.800	
$\alpha = 10^\circ + 5^\circ \sin \omega t, M = 0.295$							
0.010	NFR	NFR	67.0	67.0	66.5	63.0	21201
.025	NFR	NFR	95.0	93.5	82.0	49.0	22223
.050	NFR	NFR	69.0	66.0	61.5	57.0	22300
.100	NFR	72.0	77.5	75.5	70.0	66.0	22301
.150	68.0	76.0	82.0	76.0	81.0	85.0	22302
.200	64.0	69.5	79.0	68.5	75.0	83.0	22303
$\alpha = 15^\circ + 10^\circ \sin \omega t, M = 0.295$							
0.010	-99.9	37.5	4.5	2.5	2.5	0.0	21102
.025	0.0	3.5	3.5	3.5	3.5	5.5	17118
.050	0.5	1.5	4.5	6.5	8.0	9.5	17123
.100	10.0	12.5	14.5	15.0	19.0	20.5	17201
$\alpha = 15^\circ + 10^\circ \sin \omega t, M = 0.185$							
0.050	14.0	15.5	17.5	16.0	10.0	6.5	17102
.100	20.5	21.5	25.0	24.0	21.0	19.0	17108
.150	28.0	30.0	32.0	32.0	33.5	26.5	17110

TABLE 5.- PHASE ANGLE OF FLOW REVERSAL: Sikorsky SC-1 AIRFOIL

Mach No.	x/c						Ref. frame
	0.025	0.100	0.250	0.400	0.600	0.800	
$\alpha = 15^\circ + 10^\circ \sin \omega t, k = 0.1$							
0.076	33.5	30.5	24.5	21.0	15.5	23.5	33023
.110	43.5	41.0	28.0	28.0	36.5	42.5	33107
.185	42.0	38.0	33.0	35.0	36.5	48.5	33111
.220	32.0	28.5	26.5	24.5	28.5	35.5	33206
.250	22.0	18.5	22.5	26.0	29.5	34.5	33208
.280	15.0	14.5	18.5	20.5	23.5	27.5	33216
.295	9.0	12.0	15.0	18.0	22.5	16.5	33303
Reduced freq.	x/c						Ref. frame
	0.025	0.100	0.250	0.400	0.600	0.800	
$\alpha = 11^\circ + 5^\circ \sin \omega t, M = 0.295$							
0.050	-99.9	70.0	61.0	52.0	65.0	67.5	37220
.100	66.0	62.5	61.5	63.5	65.5	67.0	37222

TABLE 6.- PHASE ANGLE OF FLOW REVERSAL: Hughes HH-02 AIRFOIL

Mach No.	x/c						Ref. frame
	0.030	0.120	0.250	0.380	0.560	0.750	
$\alpha = 15^\circ + 10^\circ \sin \omega t, k = 0.1$							
0.076	40.0	40.0	32.5	28.0	17.5	11.5	42112
.110	48.5	45.0	40.5	36.5	30.5	13.5	42322
.185	52.5	42.0	40.0	38.5	37.0	32.4	42303
.220	25.0	25.0	28.0	31.5	36.0	15.5	42310
.250	15.0	16.0	17.0	19.5	24.5	18.0	42314
.280	7.0	9.0	11.5	13.0	14.5	5.8	42319
.295	5.0	9.5	15.1	18.5	13.0	13.0	42211
Reduced freq.	x/c						Ref. frame
	0.025	0.100	0.250	0.400	0.600	0.800	
$\alpha = 10^\circ + 5^\circ \sin \omega t, M = 0.295$							
0.010	NFR	72.0	68.5	59.0	47.5	20.5	44020
.025	NFR	78.5	74.5	60.0	49.0	33.0	44022
.050	53.5	60.0	64.5	62.5	57.0	36.5	44100
.100	58.5	67.0	78.0	79.0	84.0	50.0	44105
.150	56.0	67.0	80.0	83.5	94.0	54.0	44107
.200	57.5	67.0	79.0	86.0	94.0	58.0	44113



TABLE 7.- PHASE ANGLE OF FLOW REVERSAL: Vertol VR-7 AIRFOIL

Mach No.	x/c						Ref. frame
	0.025	0.100	0.250	0.400	0.600	0.800	
$\alpha = 15^\circ + 10^\circ \sin \omega t, k = 0.1$							
0.076	48.0	46.0	37.0	30.0	10.5	-4.0	47200
.110	51.5	49.0	44.0	32.5	15.0	-6.0	47207
.185	54.0	49.5	45.5	37.8	25.0	3.5	47214
.220	38.0	40.5	39.5	36.0	25.0	4.5	47218
.250	26.0	26.5	29.0	29.5	25.5	7.0	47302
.280	24.5	25.5	30.0	33.0	23.5	7.0	47306
.295	16.5	19.0	26.5	26.0	19.0	2.0	45100
Reduced freq.	x/c						Ref. frame
	0.025	0.010	0.250	0.400	0.600	0.800	
$\alpha = 15^\circ + 5^\circ \sin \omega t, M = 0.295$							
0.100	NFR	NFR	-3.0	-11.0	-14.0	-63.0	45204
.025	NFR	NFR	15.0	8.0	-11.0	-39.0	45206
.050	NFR	31.0	26.5	23.0	2.5	-35.0	45208
.100	NFR	36.0	36.0	30.0	17.5	-23.0	45210
.150	41.5	44.5	49.5	41.5	39.5	2.0	45212
.200	27.5	32.5	48.0	44.0	30.0	9.5	45214
$\alpha = 15^\circ + 10^\circ \sin \omega t, M = 0.295$							
0.025	NFR		14.5	18.0	6.5	-4.5	50021
.050	17.5		18.5	20.0	14.0	0.0	50019
.100	22.0		28.0	30.5	27.0	8.0	50017
.150	26.0		37.0	43.0	29.0	9.5	50015

TABLE 8.- PHASE ANGLE OF FLOW REVERSAL: NLR-1 AIRFOIL

Mach No.	x/c						Ref. frame
	0.025	0.100	0.250	0.400	0.600	0.800	
$\alpha = 15^\circ + 10^\circ \sin \omega t, k = 0.1$							
0.076	17.0	17.5	18.0	21.5	25.5	32.5	62021
.110	29.0	26.0	23.0	26.0	30.0	36.0	62105
.185	36.0	32.0	26.0	28.5	33.0	38.0	62113
.200	30.5	30.5	27.0	33.5	41.0	41.0	62115
.220	20.5	17.5	18.5	21.0	21.5	29.5	62209
.250	9.5	12.5	15.5	21.0	24.0	24.5	62211
.280	1.5	11.0	14.5	18.0	21.5	27.0	62218
.295	0.0	6.0	9.5	12.5	17.5	24.0	62308
Reduced freq.	x/c						Ref. frame
	0.025	0.100	0.250	0.400	0.600	0.800	
$\alpha = 10^\circ + 5^\circ \sin \omega t, M = 0.295$							
0.025	NFR	43.5	44.0	42.0	36.5	35.5	63109
.100	45.0	50.0	47.0	49.0	55.0	59.0	63113
.200	52.0	55.0	54.5	55.0	61.0	66.5	63115

TABLE 9.- PHASE ANGLE OF FLOW REVERSAL: NLR-7301 AIRFOIL

Mach No.	x/c						Ref. frame
	0.025	0.100	0.250	0.400	0.600	0.800	
$\alpha = 15^\circ + 10^\circ \sin \omega t, k = 0.1$							
0.110	84.0	78.5	75.0	66.5	56.0	24.0	62105
.185	98.5	93.5	82.5	76.0	50.5	35.0	62113
.250	69.5	58.5	55.0	52.5	48.0	38.5	62211
Reduced freq.	x/c						Ref. frame
	0.025	0.100	0.250	0.400	0.600	0.800	
$\alpha = 15^\circ + 5^\circ \sin \omega t, M = 0.295$							
0.010	NFR	56.5	54.5	51.0	48.5	40.5	68020
.025	NFR	64.0	57.5	53.5	48.0	16.0	68101
.050	NFR	68.5	60.0	56.5	43.5	2.0	68103
.100	NFR	34.0	43.0	44.5	43.0	11.0	68105
.150	NFR	37.5	46.0	51.0	61.0	24.0	68110
.200	NFR	35.0	53.0	64.5	44.0	23.0	68112

TABLE 10.- ERROR-BOUND FOR FLOW-REVERSAL MEASUREMENTS (deg):  
NACA 0012 AIRFOIL

Mach No.	x/c						Ref. frame
	0.025	0.100	0.250	0.400	0.600	0.800	
Corresponds to table 2: $\alpha = 15^\circ + 10^\circ \sin \omega t$ , $k = 0.1$							
0.035	4.0	0.0	1.5	1.0	1.5	2.0	8103
.073	2.0	0.0	1.5	2.5	5.0	3.0	8115
.110	1.5	0.5	0.5	1.0	3.0	3.0	2320
.145	5.0	2.5	4.0	3.5	3.5	3.5	2314
.185	0.5	2.0	1.0	1.0	3.5	2.0	8221
.185	2.5	3.0	2.5	1.5	4.0	9.0	2310
.220	3.0	1.0	0.5	2.5	2.5	3.0	2208
.250	0.0	0.0	1.5	2.0	0.5	1.5	2204
.270	2.0	2.0	2.0	2.5	1.5	0.0	2202
.280	2.0	2.0	1.0	2.0	2.0	3.0	2200
.290	0.5	2.5	1.5	2.5	1.0	1.5	2103
.295	0.5	1.5	1.5	0.0	0.0	2.5	2101
Reduced freq.	x/c						Ref. frame
	0.025	0.100	0.250	0.400	0.600	0.800	
Corresponds to table 2: $\alpha = 12^\circ + 5^\circ \sin \omega t$ , $M = 0.295$							
0.025	NFR	5.0	4.0	2.0	2.0	1.5	7201
.050	NFR	0.0	2.0	5.0	2.0	2.0	7204
.100	NFR	2.0	2.0	2.5	4.0	4.6	7206
.200	5.0	1.0	3.5	5.0	2.0	1.5	7208

ORIGINAL PAGE IS  
OF POOR QUALITY

ORIGINAL PAGE IS  
OF POOR QUALITY

TABLE 11.- ERROR-BOUND FOR FLOW-REVERSAL MEASUREMENTS (deg):  
Ames A-01 AIRFOIL

Mach No.	x/c						Ref. frame
	0.025	0.100	0.250	0.400	0.600	0.800	
Corresponds to table 3: $\alpha = 15^\circ + 10^\circ \sin \omega t$ , $k = 0.1$							
0.076	1.5	1.5	6.0	3.0	0.5	6.0	24400
.110	1.0	0.5	2.0	2.0	2.0	3.0	24316
.185	1.5	2.5	5.0	4.0	1.2	3.0	24219
.220	2.0	3.0	3.0	3.5	6.5	5.0	24210
.250	1.0	1.5	1.0	0.0	4.0	2.0	24202
.280	0.0	1.5	1.5	1.5	2.0	4.0	24118
.295	0.5	1.5	0.5	1.5	1.5	3.0	24108
Reduced freq.	x/c						Ref. frame
	0.025	0.100	0.250	0.400	0.600	0.800	
Corresponds to table 3: $\alpha = 11^\circ + 5^\circ \sin \omega t$ , $M = 0.295$							
0.010	NFR	3.0	4.0	4.0	3.5	2.5	30202
.050	NFR	6.5	2.5	2.5	2.0	5.5	25215
.100	Data too irregular to be analyzed						25217
Corresponds to table 3: $\alpha = 15^\circ + 10^\circ \sin \omega t$ , $M = 0.295$							
0.010	NFR	3.0	2.0	3.0	1.0	1.5	30021
.025	2.0	2.5	3.0	1.0	1.0	1.0	31016
.050	1.0	1.0	0.5	0.0	2.5	3.5	31018
.100	1.3	1.0	1.0	1.5	4.0	2.0	31019
.150	1.5	3.0	2.5	1.0	1.5	0.5	31020

ORIGINAL PAGE IS  
OF POOR QUALITY

TABLE 12.- ERROR-BOUND FOR FLOW-REVERSAL MEASUREMENTS (deg):  
Wortmann FX-098 AIRFOIL

Mach No.	x/c						Ref. frame
	0.025	0.100	0.250	0.400	0.600	0.800	
Corresponds to table 4: $\alpha = 15^\circ + 10^\circ \sin \omega t$ , $k = 0.1$							
0.036	0.5	1.5	0.0	1.5	1.0	1.0	16022
.076	2.0	3.0	1.5	1.0	1.0	2.0	16106
.110	1.0	2.0	3.0	1.0	1.0	1.0	16115
.185	1.0	1.0	1.0	3.0	3.0	2.0	16201
.220	1.0	1.0	1.5	2.0	2.0	3.0	16301
.250	1.5	1.0	1.0	0.5	1.5	2.0	16309
Reduced freq.	x/c						Ref. frame
	0.025	0.100	0.250	0.400	0.600	0.800	
Corresponds to table 4: $\alpha = 10^\circ + 5^\circ \sin \omega t$ , $M = 0.295$							
0.025	NFR	NFR	3.0	3.5	7.0	2.5	22223
.050	NFR	NFR	2.0	2.0	2.0	2.0	22300
.100	NFR	2.0	3.0	1.0	1.0	1.0	22301
.150	2.5	0.5	1.0	1.5	1.0	1.0	22302
.200	3.0	1.5	0.0	0.0	1.0	3.5	22303
Corresponds to table 4: $\alpha = 15^\circ + 10^\circ \sin \omega t$ , $M = 0.295$							
0.010	NFR	2.0	1.0	2.0	2.0	2.5	22102
.025	0.0	0.0	0.0	0.0	0.0	0.0	17118
.050	1.0	1.5	1.0	0.5	1.5	0.5	17123
.100	1.0	2.0	0.5	2.0	2.0	5.0	17201
Corresponds to table 4: $\alpha = 15^\circ + 10^\circ \sin \omega t$ , $M = 0.295$							
0.050	14.0	15.5	17.5	16.0	10.0	6.5	17102
.100	20.5	21.5	25.0	24.0	21.0	19.0	17108
.150	28.0	30.0	32.0	32.0	33.5	26.5	17110

ORIGINAL PAGE IS  
OF POOR QUALITY

TABLE 13.- ERROR-BOUND FOR FLOW-REVERSAL MEASUREMENTS (deg):  
Hughes HH-02 AIRFOIL

Mach No.	x/c						Ref. frame
	0.030	0.120	0.250	0.380	0.560	0.750	
Corresponds to table 6: $\alpha = 15^\circ + 10^\circ \sin \omega t$ , $k = 0.1$							
0.076	1.0	1.0	3.0	1.5	3.0	4.0	42122
.110	1.5	2.0	3.0	7.0	8.0	2.0	42322
.185	3.0	2.0	3.0	2.0	3.0	3.0	42303
.220	1.0	1.0	1.0	1.0	1.5	4.0	42310
.250	1.0	1.5	2.0	1.5	1.0	4.0	42314
.280	0.0	3.0	2.0	2.0	3.0	1.0	42319
.295	1.0	1.0	7.0	1.0	1.0	1.0	42211
Reduced freq.	x/c						Ref. frame
	0.050	0.100	0.250	0.400	0.600	0.800	
Corresponds to table 6: $\alpha = 10^\circ + 5^\circ \sin \omega t$ , $M = 0.295$							
0.010	NFR	3.5	5.0	4.5	2.5	2.0	44020
.025	NFR	6.5	6.5	3.5	3.0	3.0	44022
.050	1.0	1.5	1.5	1.5	2.0	2.0	44100
.100	2.0	0.5	2.5	2.0	2.0	2.0	44105
.150	1.0	3.0	3.0	3.0	6.5	0.0	44107
.200	1.0	1.0	0.0	1.0	2.0	5.5	44113



**ORIGINAL PAGE IS  
OF POOR QUALITY**

TABLE 15.- ERROR-BOUND FOR FLOW-REVERSAL MEASUREMENTS (deg):  
NLR-1 AIRFOIL

Mach No.	x/c						Ref. frame
	0.025	0.100	0.250	0.400	0.600	0.800	
Corresponds to table 8: $\alpha = 15^\circ + 10^\circ \sin \omega t$ , $k = 0.1$							
0.076	0.5	2.0	1.0	2.0	2.5	5.0	62021
.110	0.5	4.0	2.0	2.5	4.0	1.0	62105
.185	1.0	3.0	3.0	1.0	3.0	2.0	62113
.200	1.0	1.0	2.0	2.0	2.0	2.0	62115
.220	1.0	0.0	0.5	1.0	3.0	1.0	62209
.250	0.5	1.0	1.5	1.0	1.5	1.0	62211
.280	1.0	2.0	1.0	0.0	0.5	1.0	62218
.295	0.0	1.0	2.0	1.0	3.0	1.5	62308
Reduced freq.	x/c						Ref. frame
	0.025	0.100	0.250	0.400	0.600	0.800	
Corresponds to table 8: $\alpha = 10^\circ + 5^\circ \sin \omega t$ , $M = 0.295$							
0.025	NFR	3.5	3.0	3.5	0.5	0.5	63109
.100	0.0	0.5	5.0	2.0	2.5	2.0	63113
.200	2.0	0.5	5.5	2.0	0.0	2.5	63115

TABLE 16.- ERROR-BOUND FOR FLOW-REVERSAL MEASUREMENTS (deg):  
NLR-7301 AIRFOIL

Mach No.	x/c						Ref. frame
	0.025	0.100	0.250	0.400	0.600	0.800	
Corresponds to table 9: $\alpha = 15^\circ + 10^\circ \sin \omega t$ , $k = 0.1$							
0.110	4.0	4.0	10.0	13.0	11.0	6.0	67121
.185	5.0	6.0	7.0	7.0	4.0	1.5	67221
.250	2.5	2.5	1.0	2.0	5.0	1.1	67306
Reduced freq.	x/c						Ref. frame
	0.025	0.100	0.250	0.400	0.600	0.800	
Corresponds to table 9: $\alpha = 15^\circ + 5^\circ \sin \omega t$ , $M = 0.295$							
0.010	NFR	1.0	1.5	0.5	1.5	2.0	68020
.025	NFR	2.0	3.0	2.0	1.5	4.0	68101
.050	NFR	3.5	3.5	5.5	0.5	2.5	68103
.100	NFR	1.0	1.0	2.0	0.5	5.0	68105
.150	NFR	1.5	1.0	4.5	2.5	5.5	68110
.200	NFR	0.5	4.0	4.0	11.0	9.0	68112



ORIGINAL FRAMES  
OF POOR QUALITY

TABLE 17.- NOTES PERTAINING TO TABLES 18 TO 25

DATA LISTED IN ORDER A FRAMES STORED ON DIGITAL TAPE  
B FRAMES ARE ON ANALOG TAPE ONLY

- A FRAME - CATALOG ENTRY FOR PRESSURE DATA
- TRIP - TRIP IS PRESENT - (Y)YES, OR (N)NO
- TYPE - TEST CONDITIONS (S)STEADY, OR (U)UNSTEADY
- AO - MEAN ANGLE OF OSCILLATION, DEGREES
- A1 - AMPLITUDE OF OSCILLATION, DEGREES
- Q - FREE STREAM DYNAMIC PRESSURE, PSI
- M - FREE STREAM MACH NUMBER
- RE - FREE STREAM REYNOLDS NUMBER
- FREQ - DIMENSIONAL FREQUENCY, HERTZ
- B FRAME - CATALOG ENTRY FOR HOT-FILM AND HOT-WIRE DATA

TABLE 18.- CATALOG OF RECORDED DATA: NACA 0012 AIRFOIL

A														B															
FRAME	TRIP	TYPE	AU	A1	Q	H	RE	K	FREQ	FRAME	TRIP	TYPE	AO	A1	Q	H	RE	K	FREQ	FRAME	TRIP	TYPE	AO	A1	Q	H	RE	K	FREQ
4019	N	ST	-5.0	0.0	.875	.301	3957803.	0.0000	0.00	4020	N	US	9.0	5.0	.878	.301	3909814.	.1496	8.10	7102	N	US	9.0	5.0	.878	.301	3901884.	.0249	1.35
4100	N	ST	-2.0	0.0	.877	.301	3923537.	0.0000	0.00	4101	N	US	8.0	5.0	.878	.301	3901884.	.0250	1.35	7102	N	US	8.0	5.0	.878	.301	3901884.	.0249	1.35
4102	N	ST	0.0	0.0	.877	.301	3923848.	0.0000	0.00	4103	N	US	8.0	5.0	.878	.301	3920784.	.0250	1.35	7103	N	US	8.0	5.0	.878	.301	3903187.	.0997	5.40
4109	N	ST	2.0	0.0	.877	.302	3910221.	0.0000	0.00	4110	N	US	8.0	5.0	.877	.301	3903187.	.0997	5.40	7104	N	US	8.0	5.0	.877	.301	3903187.	.0997	5.40
4111	N	ST	4.0	0.0	.885	.299	3931136.	0.0000	0.00	4112	N	US	8.0	5.0	.877	.301	3894727.	.1992	10.80	7105	N	US	8.0	5.0	.877	.301	3894727.	.1992	10.80
4113	N	ST	8.0	0.0	.877	.302	3898235.	0.0000	0.00	4114	N	US	10.0	5.0	.877	.301	3879891.	.0252	1.37	7201	N	US	10.0	5.0	.877	.301	3879891.	.0252	1.37
4119	N	ST	10.0	0.0	.877	.301	3500632.	0.0000	0.00	4120	N	US	10.0	5.0	.877	.301	3877295.	.0994	5.40	7202	N	US	10.0	5.0	.877	.301	3877295.	.0994	5.40
4123	N	ST	12.0	0.0	.877	.302	3876047.	0.0000	0.00	4201	N	US	10.0	5.0	.877	.301	3869051.	.1987	10.80	7206	N	US	10.0	5.0	.877	.301	3869051.	.1987	10.80
4201	N	ST	13.0	0.0	.877	.302	3870568.	0.0000	0.00	4202	N	US	11.0	5.0	.878	.301	3891815.	.0249	1.35	7208	N	US	11.0	5.0	.878	.301	3891815.	.0249	1.35
4203	N	ST	13.5	0.0	.879	.301	3867132.	0.0000	0.00	4204	N	US	11.0	5.0	.878	.301	3875085.	.0497	2.70	7215	N	US	11.0	5.0	.878	.301	3875085.	.0497	2.70
4209	N	ST	14.0	0.0	.877	.302	3861326.	0.0000	0.00	4210	N	US	11.0	5.0	.877	.301	3865664.	.0993	5.40	7217	N	US	11.0	5.0	.877	.301	3865664.	.0993	5.40
4211	N	ST	14.5	0.0	.868	.305	3822671.	0.0000	0.00	4212	N	US	11.0	5.0	.877	.301	3860258.	.1488	8.10	7301	N	US	11.0	5.0	.877	.301	3860258.	.1488	8.10
4213	N	ST	15.0	0.0	.877	.302	3843407.	0.0000	0.00	4214	N	US	11.0	5.0	.878	.301	3852461.	.1983	10.80	8020	N	US	11.0	5.0	.878	.301	3852461.	.1983	10.80
4215	N	ST	15.5	0.0	.784	.284	3628769.	0.0000	0.00	4216	N	US	12.0	5.0	.878	.301	3878632.	.0249	1.35	8022	N	US	12.0	5.0	.878	.301	3878632.	.0249	1.35
4217	N	ST	16.0	0.0	.688	.266	3398340.	0.0000	0.00	4218	N	US	12.0	5.0	.877	.302	3853339.	.0991	5.40	8024	N	US	12.0	5.0	.877	.302	3853339.	.0991	5.40
4219	N	ST	17.8	0.0	.717	.271	3462550.	0.0000	0.00	4220	N	US	12.0	5.0	.877	.302	3845471.	.1981	10.80	8105	N	US	12.0	5.0	.877	.302	3845471.	.1981	10.80
4301	N	ST	20.0	0.0	.700	.266	3448278.	0.0000	0.00	4302	N	US	12.0	5.0	.877	.302	3864684.	.1488	8.10	8107	N	US	12.0	5.0	.877	.302	3864684.	.1488	8.10
4401	N	ST	13.0	0.0	.877	.302	3795037.	0.0000	0.00	4402	N	US	8.8	5.0	.877	.302	3659691.	.0992	5.40	8115	N	US	8.8	5.0	.877	.302	3659691.	.0992	5.40
4403	N	ST	11.0	0.0	.877	.302	3783629.	0.0000	0.00	4404	N	US	8.8	5.0	.877	.302	3856685.	.0496	2.70	8119	N	US	8.8	5.0	.877	.302	3856685.	.0496	2.70
4405	N	ST	8.0	0.0	.877	.302	3780176.	0.0000	0.00	4406	N	US	8.8	5.0	.877	.302	3986300.	.1513	8.10	8204	N	US	8.8	5.0	.877	.302	3986300.	.1513	8.10
4410	N	ST	5.0	0.0	.877	.302	3781319.	0.0000	0.00	4411	N	US	10.0	5.0	.877	.300	3957627.	.0745	4.00	8204	N	US	10.0	5.0	.877	.300	3957627.	.0745	4.00
4411	N	ST	2.0	0.0	.877	.302	3783016.	0.0000	0.00	4412	N	US	10.0	5.0	.877	.300	3966326.	.1510	8.10	8204	N	US	10.0	5.0	.877	.300	3966326.	.1510	8.10
4412	N	ST	0.0	0.0	.877	.302	3781623.	0.0000	0.00	4413	N	US	12.0	5.0	.877	.300	3966326.	.1510	8.10	8020	N	US	12.0	5.0	.877	.300	3966326.	.1510	8.10
4418	N	ST	-2.0	0.0	.877	.302	3778643.	0.0000	0.00	4419	N	US	10.0	10.0	.013	.035	486001.	.1515	.97	8022	N	US	10.0	10.0	.013	.035	486001.	.1515	.97
11019	N	ST	-5.0	0.0	.875	.302	3998937.	0.0000	0.00	8023	N	US	10.0	10.0	.013	.035	485752.	.2524	1.62	8024	N	US	10.0	10.0	.013	.035	485752.	.2524	1.62
11020	N	ST	-2.0	0.0	.875	.301	3869548.	0.0000	0.00	8102	N	US	15.0	10.0	.013	.036	485630.	.1032	.66	8103	N	US	15.0	10.0	.013	.036	485630.	.1032	.66
11101	N	ST	0.0	0.0	.875	.302	3978589.	0.0000	0.00	8104	N	US	15.0	10.0	.013	.036	484039.	.1529	.98	8105	N	US	15.0	10.0	.013	.036	484039.	.1529	.98
11102	N	ST	2.0	0.0	.875	.301	3958541.	0.0000	0.00	8106	N	US	15.0	14.0	.013	.036	483453.	.1039	.67	8107	N	US	15.0	14.0	.013	.036	483453.	.1039	.67
11105	N	ST	4.0	0.0	.876	.301	3938660.	0.0000	0.00	8114	N	US	15.0	10.0	.054	.072	980395.	.0992	1.30	8115	N	US	15.0	10.0	.054	.072	980395.	.0992	1.30
11110	N	ST	8.1	0.0	.875	.301	3936424.	0.0000	0.00	8116	N	US	15.0	10.0	.054	.072	979893.	.1487	1.95	8119	N	US	15.0	10.0	.054	.072	979893.	.1487	1.95
11111	N	ST	10.0	0.0	.875	.301	3926424.	0.0000	0.00	8118	N	US	15.0	10.0	.054	.072	978493.	.2477	3.25	8200	N	US	15.0	10.0	.054	.072	978493.	.2477	3.25
11112	N	ST	12.3	0.0	.875	.301	3921945.	0.0000	0.00	8123	N	US	10.0	10.0	.054	.072	980066.	.0991	1.30	8204	N	US	10.0	10.0	.054	.072	980066.	.0991	1.30
11113	N	ST	13.4	0.0	.875	.301	3912483.	0.0000	0.00	8203	N	US	10.0	10.0	.054	.072	978307.	.2476	3.25	8204	N	US	10.0	10.0	.054	.072	978307.	.2476	3.25
11118	N	ST	13.8	0.0	.875	.301	3904607.	0.0000	0.00	8210	N	US	10.0	10.0	.122	.109	1491495.	.2497	4.90	8221	N	US	10.0	10.0	.122	.109	1491495.	.2497	4.90
11121	N	ST	14.6	0.0	.875	.302	3929975.	0.0000	0.00	8214	N	US	15.0	10.0	.122	.109	1480389.	.0996	1.96	8221	N	US	15.0	10.0	.122	.109	1480389.	.0996	1.96
11122	N	ST	15.0	0.0	.887	.304	3925323.	0.0000	0.00	8220	N	US	15.0	10.0	.339	.184	2432854.	.0993	3.30	8223	N	US	15.0	10.0	.339	.184	2432854.	.0993	3.30
11200	N	ST	15.5	0.0	.811	.289	3745403.	0.0000	0.00	8222	N	US	15.0	10.0	.339	.184	2423357.	.1487	4.95	8307	N	US	15.0	10.0	.339	.184	2423357.	.1487	4.95
11201	N	ST	16.0	0.0	.811	.290	3733699.	0.0000	0.00	8306	N	US	15.0	14.0	.339	.184	2404523.	.0988	3.30	8307	N	US	15.0	14.0	.339	.184	2404523.	.0988	3.30
11204	N	ST	17.0	0.0	.841	.295	3793167.	0.0000	0.00	9022	N	US	15.0	6.0	.339	.184	2358259.	.2352	7.92	9111	N	US	15.0	6.0	.339	.184	2358259.	.2352	7.92
11205	N	ST	17.9	0.0	.803	.288	3725491.	0.0000	0.00	9101	N	US	15.0	5.0	.339	.184	2358620.	.2842	9.57	9111	N	US	15.0	5.0	.339	.184	2358620.	.2842	9.57
11205	N	ST	20.0	0.0	.764	.280	3616412.	0.0000	0.00	9106	N	US	10.0	10.0	.339	.184	2358620.	.2453	8.25	9111	N	US	10.0	10.0	.339	.184	2358620.	.2453	8.25
11208	N	ST	24.9	0.0	.610	.249	3252565.	0.0000	0.00	9110	N	US	8.0	10.0	.339	.184	2476299.	.0100	.33	9113	N	US	8.0	10.0	.339	.184	2476299.	.0100	.33
11209	N	ST	30.0	0.0	.561	.239	3105558.	0.0000	0.00	9112	N	US	8.0	10.0	.341	.183	2475104.	.0500	1.65	9113	N	US	8.0	10.0	.341	.183	2475104.	.0500	1.65
11210	N	ST	25.0	0.0	.619	.251	3254780.	0.0000	0.00	9118	N	US	8.0	10.0	.339	.184	2449160.	.1990	6.60	9119	N	US	8.0	10.0	.339	.184	2449160.	.1990	6.60
11211	N	ST	20.0	0.0	.725	.273	3515071.	0.0000	0.00	9202	N	US	15.0	10.0	.479	.220	2647551.	.0985	3.93	9119	N	US	15.0	10.0	.479	.220	2647551.	.0985	3.93
11213	N	ST	18.0	0.0	.764	.280	3628495.	0.0000	0.00	9203	N	US	15.0	10.0	.610	.249	3187113.	.0484	4.46	9119	N	US	15.0	10.0	.610	.249	3187113.	.0484	4.46
11215	N	ST	16.0	0.0	.875	.302	3866108.	0.0000	0.00	9208	N	US	15.0	10.0	.762	.280	3520275.	.0975	4.98	9119	N	US	15.0	10.0	.762	.280	3520275.	.0975	4.98
11216	N	ST	14.0	0.0	.869	.302																							

ORIGINAL PAGE IS  
OF POOR QUALITY

TABLE 18.- Concluded.

A	FRAME	TRIP	TYPE	A0	A1	Q	H	RE	K	FREQ	B	FRAME
10105	N	US	12.0	8.0	.878	.302	3694271.	.0968	5.36	12033		
10108	N	US	12.0	8.0	.847	.295	3635589.	1.253	6.81	12105		
10113	N	US	15.0	5.0	.876	.302	3896846.	.0998	5.53	12112		
10114	N	US	15.0	5.0	.841	.295	3801337.	.0252	1.34	12121		
10118	N	US	15.0	5.0	.823	.291	3748526.	10.20	5.36	12212		
10120	N	US	15.0	5.0	.845	.294	3785165.	15.11	8.04	12306		
10123	N	US	15.0	5.0	.832	.293	3758528.	20.24	10.72	13104		
10202	N	US	10.0	5.0	.877	.301	3858103.	.0098	5.54	13108		
10203	N	US	10.0	5.0	.877	.301	3847481.	.0246	1.34	13116		
10204	N	US	10.0	5.0	.870	.300	3826614.	.0493	2.68	13202		
10207	N	US	10.0	5.0	.877	.302	3884629.	.0740	4.02	13213		
10208	N	US	10.0	5.0	.870	.300	3859785.	.0990	5.36	13104		
10211	N	US	10.0	5.0	.870	.300	3863353.	1.886	8.04	12306		
10212	N	US	10.0	5.0	.870	.300	3850737.	1.979	10.72	13104		
10218	N	US	5.0	5.0	.880	.300	3933484.	.0098	5.53	12105		
10221	N	US	5.0	5.0	.878	.301	3925387.	.0993	5.36	12112		
10222	N	US	5.0	5.0	.878	.301	3912114.	1.983	10.72	12306		
10303	N	US	3.8	10.0	.877	.301	3910580.	.0991	5.36	13104		
10305	N	US	3.8	10.0	.877	.301	3911328.	.0991	5.36	13108		
10309	N	US	2.8	10.0	.877	.301	3896361.	.0989	5.36	13116		
12020	N	US	20.0	10.0	.718	.270	3490909.	.0010	.05	12105		
12102	N	US	5.0	10.0	.882	.302	3820000.	.0009	.05	12112		
12109	N	US	6.0	10.0	.756	.279	3485785.	.0010	.05	12121		
12118	N	US	20.0	10.0	.676	.262	3246704.	.0010	.05	12212		
12203	N	US	20.0	10.0	.531	.231	2887477.	.0011	.05	12306		
12208	N	US	7.0	10.0	.587	.244	3269975.	.0010	.05	13104		
12300	N	US	7.0	10.0	.421	.204	2706734.	.0011	.04	13108		
12305	N	US	20.0	10.0	.292	.169	2252844.	.0011	.03	13116		
12310	N	US	7.0	10.0	.350	.186	2469266.	.0010	.03	13202		
13021	N	US	7.0	10.0	.120	.108	1502757.	.0017	.03	13213		
13107	N	US	20.0	10.0	.113	.105	1421201.	.0017	.03	13104		
13115	N	US	20.0	10.0	.048	.068	918563.	.0027	.03	13108		
13120	N	US	5.0	10.0	.053	.072	962303.	.0025	.03	13116		
13205	N	US	5.0	10.0	.014	.036	488772.	.0025	.02	13202		
13217	N	US	5.0	10.0	.013	.036	485631.	.0026	.02	13213		
13222	N	US	20.0	10.0	.749	.276	3656957.	.0010	.05	13316		
13303	N	US	7.0	10.0	.603	.247	3298109.	.0010	.05	13405		
13308	N	US	7.0	10.0	.461	.215	2884310.	.0010	.04	14020		
13310	N	US	7.0	10.0	.466	.216	2884723.	.0010	.04	14022		
13313	Y	US	7.0	10.0	.332	.181	2404990.	.0010	.03	14100		
13321	Y	US	7.0	10.0	.339	.183	2453890.	.0009	.05	14105		
14019	Y	US	15.0	10.0	.339	.183	2434182.	.0499	1.65	14109		
14021	Y	US	15.0	10.0	.336	.182	2426579.	1.504	4.95	14118		
14023	Y	US	15.0	10.0	.335	.182	2426579.	1.504	4.95	14201		
14104	Y	US	15.0	10.0	.338	.183	2448651.	.0499	1.65	14203		
14106	Y	US	15.0	10.0	.340	.184	2449389.	.0994	3.30	14209		
14108	Y	US	15.0	10.0	.339	.183	2443079.	1.493	4.95	14211		
14117	Y	US	15.0	10.0	.837	.293	3843264.	.0257	1.35	14221		
14119	Y	US	15.0	10.0	.836	.293	3818432.	.0509	2.68	14221		
14200	Y	US	15.0	10.0	.843	.294	3822179.	.0253	1.34	14201		
14202	Y	US	15.0	10.0	.839	.293	3792702.	.0506	2.68	14203		
14208	Y	US	15.0	10.0	.828	.291	3764396.	1.019	5.36	14209		
14210	Y	US	15.0	10.0	.832	.292	3760353.	1.014	5.36	14211		
14218	N	US	15.0	10.0	.830	.292	3762798.	.0254	1.34	14221		
14219	N	US	15.0	10.0	.824	.291	3735990.	.0509	2.68	14221		
14220	N	US	15.0	10.0	.805	.287	3683317.	1.031	5.24	7201		
15218	N	US	15.0	10.0	.818	.290	3678973.	.0994	5.24	7223		
10117	N	US	15.0	5.0	.843	.295	3802563.	.0504	2.68			
7202	N	US	12.0	5.0	.877	.302	3861194.	.0496	2.70			
7222	N	US	10.0	5.0	.876	.298	3975490.	.0509	2.70			

TABLE 19.- CATALOG OF RECORDED DATA: Ames A-01 AIRFOIL

A										B																																							
FRAME	TRIP	TYPE	AO	A1	Q	M	RE	K	FREQ	FRAME	TRIP	TYPE	AO	A1	Q	M	RE	K	FREQ	FRAME																													
26020	N	ST	-5.0	0.0	880	301	3921512.	0.0000	0.00	26021	N	ST	20.0	0.0	342	184	2418525.	0.0000	0.00	27307	N	ST	20.0	0.0	342	184	2418525.	0.0000	0.00	27400	N	ST	-5.0	0.0	121	109	1538531.	0.0000	0.00	27401	N	ST	-5.0	0.0	121	109	1538531.	0.0000	0.00
26021	N	ST	-2.0	0.0	881	302	3907918.	0.0000	0.00	26022	N	ST	16.0	0.0	342	184	2422443.	0.0000	0.00	27308	N	ST	14.0	0.0	342	184	2422443.	0.0000	0.00	27401	N	ST	-2.0	0.0	121	108	1533751.	0.0000	0.00	27404	N	ST	2.0	0.0	122	109	1536087.	0.0000	0.00
26022	N	ST	0.0	0.0	882	302	3900668.	0.0000	0.00	26100	N	ST	14.0	0.0	342	184	2422443.	0.0000	0.00	27309	N	ST	16.0	0.0	342	184	2422443.	0.0000	0.00	27402	N	ST	2.0	0.0	122	109	1536087.	0.0000	0.00	27405	N	ST	2.0	0.0	122	109	1536087.	0.0000	0.00
26101	N	ST	2.0	0.0	878	302	3878703.	0.0000	0.00		N	ST	13.0	0.0	343	185	2426821.	0.0000	0.00	27310	N	ST	13.0	0.0	343	185	2426821.	0.0000	0.00	27403	N	ST	2.0	0.0	122	109	1532038.	0.0000	0.00	27406	N	ST	4.0	0.0	122	109	1532038.	0.0000	0.00
26102	N	ST	4.0	0.0	879	302	3839303.	0.0000	0.00		N	ST	11.0	0.0	339	184	2422433.	0.0000	0.00	27311	N	ST	11.0	0.0	339	184	2422433.	0.0000	0.00	27404	N	ST	2.0	0.0	122	109	1532038.	0.0000	0.00	27409	N	ST	8.0	0.0	122	110	1527387.	0.0000	0.00
26103	N	ST	8.0	0.0	880	302	3839762.	0.0000	0.00		N	ST	4.0	0.0	341	184	2422433.	0.0000	0.00	27312	N	ST	5.0	0.0	339	184	2422433.	0.0000	0.00	27405	N	ST	2.0	0.0	122	109	1532038.	0.0000	0.00	27410	N	ST	8.0	0.0	122	110	1527387.	0.0000	0.00
26104	N	ST	10.0	0.0	881	302	3826626.	0.0000	0.00		N	ST	5.0	0.0	342	184	2434809.	0.0000	0.00	27313	N	ST	5.0	0.0	342	184	2434809.	0.0000	0.00	27406	N	ST	4.0	0.0	122	109	1532038.	0.0000	0.00	27411	N	ST	10.0	0.0	121	109	1522167.	0.0000	0.00
26105	N	ST	12.0	0.0	884	303	3832104.	0.0000	0.00		N	ST	5.0	0.0	341	184	2434809.	0.0000	0.00	27314	N	ST	5.0	0.0	341	184	2434809.	0.0000	0.00	27407	N	ST	5.0	0.0	341	184	2434809.	0.0000	0.00	27412	N	ST	10.0	0.0	121	109	1522167.	0.0000	0.00
26106	N	ST	13.0	0.0	885	298	3837465.	0.0000	0.00		N	ST	13.0	0.0	342	184	2434809.	0.0000	0.00	27315	N	ST	5.0	0.0	342	184	2434809.	0.0000	0.00	27408	N	ST	5.0	0.0	341	184	2434809.	0.0000	0.00	27413	N	ST	8.0	0.0	122	110	1527387.	0.0000	0.00
26107	N	ST	13.5	0.0	833	293	3667954.	0.0000	0.00		N	ST	13.5	0.0	343	185	2426376.	0.0000	0.00	27316	N	ST	13.0	0.0	343	185	2426376.	0.0000	0.00	27409	N	ST	8.0	0.0	122	110	1527387.	0.0000	0.00	27414	N	ST	10.0	0.0	121	109	1522167.	0.0000	0.00
26205	N	ST	14.0	0.0	857	298	3720572.	0.0000	0.00		N	ST	14.0	0.0	342	184	2426376.	0.0000	0.00	27317	N	ST	14.0	0.0	342	184	2426376.	0.0000	0.00	27410	N	ST	12.0	0.0	122	110	1525614.	0.0000	0.00	27415	N	ST	12.0	0.0	122	110	1525614.	0.0000	0.00
26207	N	ST	15.0	0.0	882	302	3754105.	0.0000	0.00		N	ST	15.0	0.0	343	185	2426376.	0.0000	0.00	27318	N	ST	15.0	0.0	343	185	2426376.	0.0000	0.00	27411	N	ST	12.0	0.0	122	110	1525614.	0.0000	0.00	27416	N	ST	12.0	0.0	122	110	1525614.	0.0000	0.00
26209	N	ST	16.0	0.0	870	300	3715585.	0.0000	0.00		N	ST	16.0	0.0	343	185	2426376.	0.0000	0.00	27319	N	ST	16.0	0.0	343	185	2426376.	0.0000	0.00	27412	N	ST	12.0	0.0	122	110	1525614.	0.0000	0.00	27417	N	ST	12.0	0.0	122	110	1525614.	0.0000	0.00
26215	N	ST	18.0	0.0	815	290	3589962.	0.0000	0.00		N	ST	18.0	0.0	343	185	2426376.	0.0000	0.00	27320	N	ST	18.0	0.0	343	185	2426376.	0.0000	0.00	27413	N	ST	8.0	0.0	122	110	1527387.	0.0000	0.00	27418	N	ST	13.0	0.0	121	109	1491021.	0.0000	0.00
26216	N	ST	20.0	0.0	778	282	3497091.	0.0000	0.00		N	ST	20.0	0.0	343	185	2426376.	0.0000	0.00	27321	N	ST	20.0	0.0	343	185	2426376.	0.0000	0.00	27414	N	ST	14.0	0.0	121	109	1491021.	0.0000	0.00	27419	N	ST	14.0	0.0	121	109	1491021.	0.0000	0.00
26218	N	ST	25.0	0.0	626	252	3129086.	0.0000	0.00		N	ST	25.0	0.0	343	185	2426376.	0.0000	0.00	27322	N	ST	25.0	0.0	343	185	2426376.	0.0000	0.00	27415	N	ST	15.0	0.0	132	114	1541856.	0.0000	0.00	27420	N	ST	15.0	0.0	132	114	1541856.	0.0000	0.00
26219	N	ST	20.0	0.0	773	281	3465882.	0.0000	0.00		N	ST	20.0	0.0	343	185	2426376.	0.0000	0.00	27323	N	ST	20.0	0.0	343	185	2426376.	0.0000	0.00	27416	N	ST	15.0	0.0	132	114	1541856.	0.0000	0.00	27421	N	ST	15.0	0.0	132	114	1541856.	0.0000	0.00
26220	N	ST	14.0	0.0	832	293	3591634.	0.0000	0.00		N	ST	14.0	0.0	343	185	2426376.	0.0000	0.00	26222	N	ST	16.0	0.0	341	184	2426376.	0.0000	0.00	27417	N	ST	16.0	0.0	129	112	1526677.	0.0000	0.00	27422	N	ST	16.0	0.0	129	112	1526677.	0.0000	0.00
26300	N	ST	13.0	0.0	878	302	3703082.	0.0000	0.00		N	ST	13.0	0.0	343	185	2426376.	0.0000	0.00	26314	N	ST	14.0	0.0	341	184	2441392.	0.0000	0.00	27418	N	ST	16.0	0.0	124	110	1492163.	0.0000	0.00	27423	N	ST	16.0	0.0	124	110	1492163.	0.0000	0.00
26301	N	ST	13.0	0.0	828	293	3590546.	0.0000	0.00		N	ST	13.0	0.0	343	185	2426376.	0.0000	0.00	26315	N	ST	14.0	0.0	341	184	2441392.	0.0000	0.00	27419	N	ST	16.0	0.0	124	110	1492163.	0.0000	0.00	27424	N	ST	16.0	0.0	124	110	1492163.	0.0000	0.00
26302	N	ST	11.0	0.0	879	302	3693921.	0.0000	0.00		N	ST	11.0	0.0	343	185	2426376.	0.0000	0.00	26316	N	ST	14.0	0.0	341	184	2441392.	0.0000	0.00	27420	N	ST	16.0	0.0	124	110	1492163.	0.0000	0.00	27425	N	ST	16.0	0.0	124	110	1492163.	0.0000	0.00
26306	N	ST	5.0	0.0	883	303	3706075.	0.0000	0.00		N	ST	5.0	0.0	343	185	2426376.	0.0000	0.00	26317	N	ST	14.0	0.0	341	184	2441392.	0.0000	0.00	27421	N	ST	16.0	0.0	124	110	1492163.	0.0000	0.00	27426	N	ST	16.0	0.0	124	110	1492163.	0.0000	0.00
26307	N	ST	0.0	0.0	878	302	3693264.	0.0000	0.00		N	ST	0.0	0.0	343	185	2426376.	0.0000	0.00	26318	N	ST	14.0	0.0	341	184	2441392.	0.0000	0.00	27422	N	ST	16.0	0.0	124	110	1492163.	0.0000	0.00	27427	N	ST	16.0	0.0	124	110	1492163.	0.0000	0.00
26313	N	ST	-5.0	0.0	614	250	3126375.	0.0000	0.00		N	ST	-5.0	0.0	343	185	2426376.	0.0000	0.00	26319	N	ST	14.0	0.0	341	184	2441392.	0.0000	0.00	27423	N	ST	16.0	0.0	124	110	1492163.	0.0000	0.00	27428	N	ST	16.0	0.0	124	110	1492163.	0.0000	0.00
26315	N	ST	-2.0	0.0	612	250	3113134.	0.0000	0.00		N	ST	-2.0	0.0	343	185	2426376.	0.0000	0.00	26319	N	ST	14.0	0.0	341	184	2441392.	0.0000	0.00	27424	N	ST	16.0	0.0	124	110	1492163.	0.0000	0.00	27429	N	ST	16.0	0.0	124	110	1492163.	0.0000	0.00
26318	N	ST	0.0	0.0	616	250	3132011.	0.0000	0.00																																								

TABLE 19.- Concluded.

A		B		K		M		Q		A0		A1		RE		FREQ		FRAME		
FRAME	TRIP	TYPE	US	US	US	US	US	US	US	US	US	US	US	US	US	US	US	US	US	US
25102	N	US	10.0	10.0	881	302	3831527.	.0489	2.68	25103										
25104	N	US	10.0	10.0	880	302	3816708.	.0978	5.36	25108										
25109	N	US	10.0	10.0	879	302	3810775.	1.468	8.04	25110										
25117	N	US	10.0	5.0	884	303	3829075.	0.244	1.34											
25118	N	US	10.0	5.0	879	302	3803407.	0.489	2.68											
25119	N	US	10.0	5.0	883	303	3805390.	0.975	5.36											
25121	N	US	10.0	5.0	881	302	3813088.	1.465	8.04											
25122	N	US	10.0	5.0	884	303	3819823.	1.462	8.04											
25123	N	US	10.0	5.0	885	303	3816827.	1.947	10.72											
29023	Y	US	15.0	10.0	820	291	3697799.	0.248	1.34	29100										
29101	Y	US	15.0	10.0	805	288	3639654.	0.500	2.62	29102										
29106	Y	US	15.0	10.0	806	288	3646183.	1.001	5.24	29107										
29115	Y	US	15.0	10.0	340	184	2418131.	0.494	1.65	29116										
29117	Y	US	15.0	10.0	341	184	2418248.	0.987	3.30	29118										
29119	Y	US	15.0	10.0	341	184	2417060.	1.481	4.95	29121										
29205	N	US	5.0	10.0	876	301	3947215.	0.098	5.3	29206										
29207	N	US	5.0	10.0	877	301	3918856.	0.496	2.68	29210										
29211	N	US	5.0	10.0	877	301	3902857.	0.991	5.36	29212										
29213	N	US	5.0	10.0	879	301	3896095.	1.483	8.04	29214										
29215	N	US	5.0	10.0	879	301	3891313.	1.481	8.04											
29223	N	US	13.5	2.0	876	301	3811877.	1.965	10.72	29300										
29304	N	US	14.5	2.0	870	300	3777473.	1.967	10.72	29306										
29309	N	US	15.5	2.0	852	296	3722411.	1.986	10.72	29310										
29317	N	US	15.0	10.0	013	035	472349.	1.021	6.5	29318										
30019	N	US	15.0	10.0	865	298	3856941.	0.097	5.2	30021										
30020	N	US	15.0	10.0	864	298	3828146.	0.096	5.2	30021										
30105	N	US	10.0	10.0	880	301	3844592.	0.097	5.3	30106										
30110	N	US	15.0	5.0	877	301	3817844.	0.097	5.3	30111										
30119	N	US	10.0	5.0	874	300	3819252.	0.097	5.3	30120										
30201	N	US	11.0	5.0	877	301	3814196.	0.099	5.4	30202										
30206	N	US	14.0	2.0	876	301	3818960.	0.097	5.3	30208										
30215	N	US	7.5	10.0	338	183	2415733.	0.099	3.3	30216										
31102	N	US	10.0	10.0	877	302	3880208.	0.247	1.34	31103										
31104	N	US	10.0	10.0	878	302	3859857.	0.492	2.68	31105										
31110	N	US	10.0	10.0	880	302	3841535.	1.471	8.04	31111										
31112	N	US	10.0	10.0	880	302	3832051.	1.469	8.04	31111										
31119	N	US	5.0	10.0	884	303	3856266.	0.245	1.34	31120										
31121	N	US	5.0	10.0	880	302	3826984.	0.489	2.68	31122										
31123	N	US	5.0	10.0	884	303	3823741.	0.975	5.36	31200										
31201	N	US	5.0	10.0	883	303	3816823.	1.463	8.04	31202										
31209	N	US	15.0	10.0	341	184	2421425.	0.987	3.30	31210										
31215	N	US	7.5	10.0	341	184	2425489.	0.494	1.65	31216										
31217	N	US	7.5	10.0	341	185	2423083.	1.972	6.60	31218										
31302	N	US	14.5	2.0	852	297	3765532.	1.990	10.72	31304										
31310	N	US	14.5	2.0	854	298	3731989.	1.485	8.04	31312										
25204	N	US	15.0	5.0	877	301	3973275.	0.249	1.34											
25205	N	US	15.0	5.0	878	301	3952662.	0.497	2.68											
25208	N	US	15.0	5.0	878	301	3950602.	0.994	5.36											
25209	N	US	15.0	5.0	852	298	3887313.	1.506	8.04											
25210	N	US	15.0	5.0	852	297	3865306.	2.013	10.72											
25214	N	US	11.0	5.0	880	302	3926436.	0.495	2.68	25215										
25216	N	US	11.0	5.0	883	302	3909711.	0.986	5.36	25217										
25301	N	US	5.0	5.0	884	302	3903998.	0.984	5.36	25302										
25303	N	US	5.0	5.0	885	303	3878688.	1.962	10.72	25304										
25311	N	US	5.0	10.1	881	302	3852707.	0.982	5.36	25312										
25319	N	US	5.5	10.0	881	302	3833693.	0.980	5.36	25320										



TABLE 20.- Concluded.

A	FRAME	TRIP	Y	TYPE	A0	A1	Q	M	RE	K	FREQ	B
17200	N	UN	15.0	10.0	814	.290	3702477.	.0999	5.24	21102		
21100	N	UN	15.0	10.0	.823	.291	3718613.	.0098	.52	21201		
21107	N	UN	10.0	10.0	.867	.299	3792469.	.0098	.53	21209		
21200	N	UN	10.0	5.0	.875	.301	3932117.	.0097	.53	21220		
21208	N	UN	3.3	10.0	.882	.302	3898549.	.0098	.33	22104		
21219	N	UN	6.5	10.0	.339	.184	2455459.	.0247	1.31	22207		
22023	N	UN	15.0	10.0	.827	.293	3727983.	.0492	2.62	22209		
22103	N	UN	15.0	10.0	.837	.294	3749080.	.1008	5.24			
22201	N	UN	15.0	10.0	.785	.285	3554419.	.1542	7.86			
22206	N	UN	15.0	10.0	.754	.279	3477029.	.0969	4.98			
22208	N	UN	15.0	10.0	.763	.281	3483672.	.0243	1.34			
22216	N	UN	10.0	10.0	.875	.302	3732111.	.0485	2.68			
22217	N	UN	10.0	10.0	.875	.302	3720266.	.0485	2.68			
22218	N	UN	10.0	10.0	.862	.300	3684571.	.0977	5.36			
22219	N	UN	10.0	10.0	.835	.294	3618609.	.1490	8.04			
22307	N	UN	10.0	5.0	.875	.301	3854387.	.0246	1.34	22223		
22308	N	UN	10.0	5.0	.880	.303	3857324.	.0491	2.68	22300		
22309	N	UN	10.0	5.0	.881	.303	3853461.	.0980	5.36	22301		
22311	N	UN	10.0	5.0	.877	.302	3849798.	.1475	8.04	22302		
22312	N	UN	10.0	5.0	.882	.303	3849072.	.1957	10.72	22303		
23021	N	UN	15.0	5.0	.858	.298	3792196.	.0248	1.34			
23022	N	UN	15.0	5.0	.851	.297	3750472.	.0497	2.68			
23023	N	UN	15.0	5.0	.840	.295	3716891.	.1000	5.36			
23100	N	UN	15.0	5.0	.822	.292	3670934.	.1516	8.04	23108		
23107	N	UN	5.0	5.0	.867	.300	3802836.	.0986	5.36	23110		
23109	N	UN	5.0	5.0	.867	.300	3769174.	.1970	10.72	23118		
23117	N	UN	5.0	10.0	.869	.300	3803440.	.0985	5.36	23202		
23201	N	UN	3.8	10.0	.866	.299	3948210.	.1003	5.36	23207		
23206	N	UN	3.3	10.0	.866	.299	3924045.	.0500	2.68	23210		
23208	N	UN	3.3	10.0	.871	.300	3914485.	.0996	5.36	23212		
23211	N	UN	3.3	10.0	.870	.300	3896319.	.1492	8.04	23220		
23219	N	UN	12.0	2.0	.864	.299	3865609.	.1994	10.72	23306		
23305	N	UN	14.0	2.0	.858	.298	3831711.	.1995	10.72	23311		
23310	N	UN	16.0	2.0	.839	.294	3768762.	.2014	10.72			
21112	N	UN	15.0	5.0	.873	.301	3940131.	.0099	.53			
23101	N	UN	15.0	5.0	.800	.287	3617353.	.2049	10.72			





TABLE 21.- Concluded.

A		B								
FRAME	TRIP	TYPE	AO	A1	Q	M	RE	K	FREQ	FRAME
39110	N	UN	11.0	5.0	.869	.299	3896687.	.0099	.53	
39115	N	UN	14.0	2.0	.865	.298	3838622.	.0100	.54	
38110	N	UN	16.0	2.0	.832	.293	3754517.	.2023	10.72	38111
39107	N	UN	10.0	5.0	.876	.300	3939495.	.0098	.53	

TABLE 22.- CATALOG OF RECORDED DATA: Hughes HH-02 AIRFOIL

A		B		A		B		A		B		A		B						
FRAME	TRIP	TYPE	A0	A1	Q	M	RE	K	FREQ	FRAME	TRIP	TYPE	A0	A1	Q	M	RE	K	FREQ	FRAME
40018	N	ST	-5.0	0.0	122	110	1508746.	0.0000	0.00	41215	N	ST	0.0	0.0	611	249	3331668.	0.0000	0.00	41222
40019	N	ST	0.0	0.0	121	109	1502749.	0.0000	0.00	41221	Y	ST	0.0	0.0	875	299	4054062.	0.0000	0.00	41300
40020	N	ST	5.0	0.0	123	110	1511661.	0.0000	0.00	41223	Y	ST	5.0	0.0	874	300	4025612.	0.0000	0.00	41302
40101	N	ST	10.0	0.0	123	110	1511504.	0.0000	0.00	41301	Y	ST	10.0	0.0	877	300	4012119.	0.0000	0.00	41302
40102	N	ST	12.0	0.0	120	109	1490668.	0.0000	0.00	41303	Y	ST	12.0	0.0	873	300	3995297.	0.0000	0.00	41304
40103	N	ST	14.0	0.0	125	111	1514773.	0.0000	0.00	41305	Y	ST	13.0	0.0	858	296	3950234.	0.0000	0.00	41306
40104	N	ST	14.5	0.0	123	109	1502336.	0.0000	0.00	41307	Y	ST	13.5	0.0	879	300	3987094.	0.0000	0.00	41308
40105	N	ST	15.0	0.0	122	110	1499223.	0.0000	0.00	41312	Y	ST	14.0	0.0	876	300	3990589.	0.0000	0.00	41313
40106	N	ST	15.5	0.0	121	109	1494155.	0.0000	0.00	41314	Y	ST	16.0	0.0	811	287	3822102.	0.0000	0.00	41315
40107	N	ST	16.0	0.0	121	109	1487366.	0.0000	0.00	41401	Y	ST	0.0	0.0	336	182	2505262.	0.0000	0.00	41402
40108	N	ST	20.0	0.0	122	110	1497097.	0.0000	0.00	41403	Y	ST	5.0	0.0	340	184	2516822.	0.0000	0.00	41404
40114	N	ST	-5.0	0.0	342	185	2477234.	0.0000	0.00	41405	Y	ST	10.0	0.0	339	183	2509654.	0.0000	0.00	41406
40115	N	ST	0.0	0.0	341	185	2468667.	0.0000	0.00	41407	Y	ST	12.0	0.0	336	182	2495906.	0.0000	0.00	41408
40117	N	ST	4.0	0.0	341	185	2469822.	0.0000	0.00	41409	Y	ST	13.0	0.0	337	183	2499130.	0.0000	0.00	41410
40201	N	ST	9.0	0.0	341	185	2478173.	0.0000	0.00	41411	Y	ST	13.5	0.0	333	182	2498901.	0.0000	0.00	41412
40203	N	ST	12.0	0.0	343	185	2480399.	0.0000	0.00	41413	Y	ST	14.0	0.0	334	181	2488812.	0.0000	0.00	41414
40205	N	ST	14.0	0.0	341	185	2474050.	0.0000	0.00	41415	Y	ST	14.5	0.0	339	183	2503241.	0.0000	0.00	41416
40207	N	ST	14.5	0.0	344	186	2483787.	0.0000	0.00	41417	Y	ST	16.0	0.0	338	182	2496014.	0.0000	0.00	41418
40212	N	ST	15.0	0.0	340	185	2474314.	0.0000	0.00	41419	Y	ST	0.0	0.0	338	182	2495914.	0.0000	0.00	41418
40215	N	ST	16.0	0.0	340	185	2473125.	0.0000	0.00	42019	Y	US	15.0	10.0	836	292	3952553.	0.252	1.31	42020
40222	N	ST	8.0	0.0	879	302	4129994.	0.0000	0.00	42021	Y	US	15.0	10.0	821	289	3884045.	0.0508	2.62	42022
40223	N	ST	10.0	0.0	874	301	4103323.	0.0000	0.00	42100	Y	US	15.0	10.0	788	283	3786236.	0.1035	5.24	42101
40301	N	ST	12.0	0.0	869	300	4085502.	0.0000	0.00	42108	Y	US	15.0	10.0	339	183	2530006.	0.0506	1.65	42109
40303	N	ST	13.0	0.0	875	299	4051531.	0.0000	0.00	42110	Y	US	15.0	10.0	338	183	2526566.	0.1013	3.30	42112
40308	N	ST	13.5	0.0	878	301	4059676.	0.0000	0.00	42113	Y	US	15.0	10.0	340	183	2532492.	0.1516	4.95	42114
40310	N	ST	14.0	0.0	878	301	4041789.	0.0000	0.00	42121	N	US	15.0	10.0	054	072	1027532.	0.1011	1.30	42122
40312	N	ST	14.5	0.0	883	302	4039947.	0.0000	0.00	42206	N	US	15.0	10.0	823	290	3980979.	0.0256	1.31	42207
40314	N	ST	15.0	0.0	884	303	4032069.	0.0000	0.00	42208	N	US	15.0	10.0	834	292	3977572.	0.0507	2.62	42209
40321	N	ST	18.0	0.0	806	288	3854130.	0.0000	0.00	42212	N	US	15.0	10.0	813	288	3911977.	0.1025	5.24	42211
40322	N	ST	14.0	0.0	715	270	3619314.	0.0000	0.00	42217	N	US	15.0	10.0	786	283	3830288.	0.1561	7.85	42213
40323	N	ST	13.0	0.0	869	301	4009498.	0.0000	0.00	42218	N	US	15.0	10.0	759	278	3756013.	0.1008	4.98	42219
40400	N	ST	5.0	0.0	871	299	3981644.	0.0000	0.00	42302	N	US	15.0	10.0	339	183	2526382.	0.1011	3.30	42303
40406	N	ST	5.0	0.0	877	300	3981021.	0.0000	0.00	42309	N	US	15.0	10.0	476	218	2981460.	0.1011	3.30	42310
40407	N	ST	0.0	0.0	878	301	4024289.	0.0000	0.00	43013	N	US	15.0	10.0	604	246	3327957.	0.1013	4.46	42314
41019	N	ST	-5.0	0.0	874	300	4148783.	0.0000	0.00	43211	N	US	10.0	10.0	120	108	1510607.	0.1013	1.96	42322
41021	N	ST	-2.0	0.0	872	300	4123880.	0.0000	0.00	43215	N	US	10.0	10.0	858	297	3898111.	0.1011	5.4	43220
41100	N	ST	0.0	0.0	875	300	4107145.	0.0000	0.00	43106	N	US	10.0	10.0	870	301	3930420.	0.0249	1.34	43107
41103	N	ST	5.0	0.0	877	301	4090950.	0.0000	0.00	43108	N	US	10.0	10.0	876	302	3927336.	0.0496	2.68	43109
41110	N	ST	-5.0	0.0	610	248	3409824.	0.0000	0.00	43114	N	US	10.0	10.0	861	299	3899487.	0.1502	8.04	43110
41112	N	ST	0.0	0.0	611	248	3397141.	0.0000	0.00	43117	N	US	10.0	10.0	849	297	3886604.	0.1514	8.04	43118
41114	N	ST	2.0	0.0	611	248	3391537.	0.0000	0.00	43202	N	US	3.8	10.0	874	301	3946814.	0.0249	1.34	43203
41119	N	ST	5.0	0.0	609	248	3381054.	0.0000	0.00	43204	N	US	10.0	10.0	876	302	3945527.	0.0993	5.36	43205
41120	N	ST	8.0	0.0	609	248	3361029.	0.0000	0.00	43206	N	US	3.8	10.0	876	302	3962955.	0.0497	2.68	43208
41122	N	ST	12.0	0.0	609	248	3342575.	0.0000	0.00	43209	N	US	3.8	10.0	878	302	3955351.	0.0994	5.36	43208
41200	N	ST	14.0	0.0	611	249	3329347.	0.0000	0.00	43215	N	US	3.8	10.0	876	302	3955884.	0.1489	8.04	43210
41201	N	ST	14.5	0.0	610	248	3321682.	0.0000	0.00	43219	N	US	4.0	10.0	879	303	4045707.	0.0101	5.4	43216
41202	N	ST	15.0	0.0	609	248	3317576.	0.0000	0.00	43303	N	US	15.0	5.0	821	296	3841831.	0.0254	1.34	44020
41205	N	ST	18.0	0.0	608	248	3317288.	0.0000	0.00	43305	N	US	15.0	5.0	817	291	3822850.	0.1030	5.36	44021
41206	N	ST	20.0	0.0	608	248	3306088.	0.0000	0.00	43309	N	US	15.0	5.0	805	289	3776817.	0.2073	10.72	44022
41208	N	ST	13.0	0.0	609	248	3321536.	0.0000	0.00	43314	N	US	11.0	5.0	876	302	3934345.	0.0248	1.34	44023
41209	N	ST	12.5	0.0	613	249	3319411.	0.0000	0.00	43316	N	US	11.0	5.0	877	302	3922072.	0.0489	2.65	44100
41214	N	ST	5.0	0.0	613	249	3342074.	0.0000	0.00	43319	N	US	10.0	5.0	869	301	3902929.	0.0990	5.36	44105
										44104	N	US	10.0	5.0	876	302	3943793.	0.0496	2.68	44100
										44106	N	US	10.0	5.0	881	303	3996291.	0.0993	5.36	44105
															880	303	3991389.	0.1490	8.04	44107



TABLE 23.- CATALOG OF RECORDED DATA: Vertol VR-7 AIRFOIL

A		B		A		B		A		B		A		B					
FRAME	TRIP	TYPE	AO	A1	Q	M	RE	K	FREQ	FRAME	TRIP	TYPE	AO	A1	Q	M	RE	K	FREQ
46018	N	ST	-5.0	0.0	.121	108	1551001.	0.0000	0.00	46609	N	ST	13.0	0.0	.876	299	4071175.	0.0000	0.00
46019	N	ST	0.0	0.0	.121	108	1546271.	0.0000	0.00	46610	N	ST	12.0	0.0	.881	299	4055190.	0.0000	0.00
46020	N	ST	5.0	0.0	.123	109	1557517.	0.0000	0.00	46615	N	ST	0.0	0.0	.881	300	4097411.	0.0000	0.00
46101	N	ST	10.0	0.0	.118	107	1512690.	0.0000	0.00	46621	Y	ST	0.0	0.0	.876	183	2522757.	0.0000	0.00
46102	N	ST	12.0	0.0	.122	109	1540066.	0.0000	0.00	46623	Y	ST	5.0	0.0	.340	183	2514978.	0.0000	0.00
46103	N	ST	12.5	0.0	.123	109	1547844.	0.0000	0.00	46701	Y	ST	10.0	0.0	.340	183	2513421.	0.0000	0.00
46104	N	ST	13.0	0.0	.123	109	1543789.	0.0000	0.00	46703	Y	ST	12.0	0.0	.341	183	2515338.	0.0000	0.00
46105	N	ST	13.5	0.0	.123	109	1542255.	0.0000	0.00	46705	Y	ST	13.0	0.0	.340	183	2506104.	0.0000	0.00
46106	N	ST	14.0	0.0	.122	109	1535872.	0.0000	0.00	46707	Y	ST	14.0	0.0	.338	182	2501582.	0.0000	0.00
46107	N	ST	15.0	0.0	.122	109	1537932.	0.0000	0.00	46714	Y	ST	15.0	0.0	.340	183	2518275.	0.0000	0.00
46108	N	ST	17.0	0.0	.123	109	1541148.	0.0000	0.00	46716	Y	ST	16.0	0.0	.341	184	2516975.	0.0000	0.00
46109	N	ST	20.0	0.0	.122	109	1534206.	0.0000	0.00	46718	Y	ST	20.0	0.0	.343	184	2517610.	0.0000	0.00
46110	N	ST	25.0	0.0	.120	108	1523001.	0.0000	0.00	46719	Y	ST	0.0	0.0	.342	183	2519323.	0.0000	0.00
46116	N	ST	-5.0	0.0	.341	184	2550698.	0.0000	0.00	46802	Y	ST	0.0	0.0	.881	300	4204772.	0.0000	0.00
46117	N	ST	0.0	0.0	.342	183	2552563.	0.0000	0.00	46804	Y	ST	5.0	0.0	.881	300	4185103.	0.0000	0.00
46119	N	ST	5.0	0.0	.341	183	2546869.	0.0000	0.00	46806	Y	ST	10.0	0.0	.886	301	4170536.	0.0000	0.00
46203	N	ST	10.0	0.0	.343	184	2562110.	0.0000	0.00	46808	Y	ST	12.0	0.0	.882	300	4148330.	0.0000	0.00
46205	N	ST	12.0	0.0	.341	183	2551368.	0.0000	0.00	46810	Y	ST	13.0	0.0	.883	301	4139718.	0.0000	0.00
46207	N	ST	12.5	0.0	.342	183	2553262.	0.0000	0.00	46815	Y	ST	14.0	0.0	.881	300	4137342.	0.0000	0.00
46209	N	ST	13.0	0.0	.342	184	2553793.	0.0000	0.00	46817	Y	ST	15.0	0.0	.877	300	4108330.	0.0000	0.00
46211	N	ST	13.5	0.0	.341	183	2550511.	0.0000	0.00	46819	Y	ST	16.0	0.0	.877	299	4091352.	0.0000	0.00
46217	N	ST	14.0	0.0	.342	183	2637541.	0.0000	0.00	46821	Y	ST	20.0	0.0	.806	287	3898404.	0.0000	0.00
46219	N	ST	15.0	0.0	.341	183	2630320.	0.0000	0.00	46823	Y	ST	0.0	0.0	.881	300	4085157.	0.0000	0.00
46221	N	ST	17.0	0.0	.340	183	2624424.	0.0000	0.00	45019	N	UN	15.0	10.0	.873	300	4062142.	0.0000	0.00
46223	N	ST	20.0	0.0	.340	183	2622591.	0.0000	0.00	45021	N	UN	15.0	10.0	.830	292	3937973.	0.0505	2.62
46301	N	ST	25.0	0.0	.340	183	2614669.	0.0000	0.00	45023	N	UN	15.0	10.0	.835	293	3931111.	1.0055	5.24
46307	N	ST	-5.0	0.0	.612	248	3482182.	0.0000	0.00	45109	N	UN	15.0	10.0	.793	301	3824874.	1549	7.86
46308	N	ST	-2.0	0.0	.613	249	3476509.	0.0000	0.00	45111	N	UN	10.0	10.0	.873	301	4033486.	0.101	54
46309	N	ST	0.0	0.0	.612	248	3468801.	0.0000	0.00	45113	N	UN	10.0	10.0	.875	301	4010614.	0.251	1.34
46310	N	ST	2.0	0.0	.611	248	3461144.	0.0000	0.00	45113	N	UN	10.0	10.0	.878	301	4010372.	0.500	2.68
46311	N	ST	5.0	0.0	.614	248	3462655.	0.0000	0.00	45119	N	UN	10.0	10.0	.875	301	4019136.	1.003	5.36
46317	N	ST	8.0	0.0	.615	249	3457898.	0.0000	0.00	45209	N	UN	15.0	5.0	.869	300	4015256.	1498	8.04
46318	N	ST	10.0	0.0	.611	248	3435015.	0.0000	0.00	45205	N	UN	15.0	5.0	.876	301	4008473.	0.250	1.34
46319	N	ST	12.0	0.0	.613	248	3433344.	0.0000	0.00	45207	N	UN	15.0	5.0	.877	301	4005939.	0.500	2.68
46320	N	ST	12.5	0.0	.615	249	3429825.	0.0000	0.00	45209	N	UN	15.0	5.0	.871	300	3986080.	1.002	5.36
46321	N	ST	13.0	0.0	.612	248	3419429.	0.0000	0.00	45211	N	UN	15.0	5.0	.860	298	3957187.	1513	8.04
46322	N	ST	13.5	0.0	.610	248	3409796.	0.0000	0.00	45213	N	UN	15.0	5.0	.841	295	3908733.	2041	10.72
46323	N	ST	14.0	0.0	.613	249	3417715.	0.0000	0.00	45221	N	UN	10.0	5.0	.878	302	4054475.	0.251	1.34
46400	N	ST	15.0	0.0	.613	249	3413348.	0.0000	0.00	45223	N	UN	10.0	5.0	.877	301	4032781.	0.501	2.68
46403	N	ST	17.0	0.0	.616	249	3427697.	0.0000	0.00	45300	N	UN	10.0	5.0	.878	301	4031948.	1.001	5.36
46404	N	ST	20.0	0.0	.615	249	3412222.	0.0000	0.00	45302	N	UN	10.0	5.0	.879	302	4030474.	1.500	8.04
46405	N	ST	25.0	0.0	.614	248	3396768.	0.0000	0.00	45303	N	UN	10.0	5.0	.878	301	4026973.	2.002	10.72
46406	N	ST	13.0	0.0	.613	249	3398737.	0.0000	0.00	47020	Y	UN	15.0	10.0	.859	299	4059175.	0.249	1.31
46407	N	ST	12.0	0.0	.610	248	3391942.	0.0000	0.00	47100	Y	UN	15.0	10.0	.838	292	3928981.	0.249	1.31
46412	N	ST	0.0	0.0	.614	248	3394265.	0.0000	0.00	47110	Y	UN	15.0	10.0	.820	292	3927997.	1014	5.24
46418	N	ST	-5.0	0.0	.877	300	3996105.	0.0000	0.00	47112	Y	UN	15.0	10.0	.842	185	2577901.	0508	1.65
46420	N	ST	-2.0	0.0	.878	301	3986471.	0.0000	0.00	47114	Y	UN	15.0	10.0	.842	185	2586091.	1008	3.30
46423	N	ST	2.0	0.0	.875	300	3968964.	0.0000	0.00	47116	Y	UN	15.0	10.0	.842	185	2580642.	1512	4.95
46500	N	ST	5.0	0.0	.877	300	3965878.	0.0000	0.00	47123	N	UN	15.0	10.0	.854	073	1030887.	1007	1.30
46508	N	ST	8.0	0.0	.878	300	4161706.	0.0000	0.00	47206	N	UN	15.0	10.0	.123	110	1553432.	1006	1.96
46509	N	ST	10.0	0.0	.876	299	4119351.	0.0000	0.00	47213	N	UN	15.0	10.0	.340	185	2608965.	1016	3.30
46511	N	ST	12.0	0.0	.876	299	4119351.	0.0000	0.00	47217	N	UN	15.0	10.0	.479	221	3036397.	1008	3.93
46513	N	ST	12.5	0.0	.874	299	4099803.	0.0000	0.00	47301	N	UN	15.0	10.0	.610	250	3408483.	1009	4.46
46515	N	ST	13.0	0.0	.867	298	4070743.	0.0000	0.00	47305	N	UN	15.0	10.0	.760	281	3783711.	1003	4.98
46517	N	ST	13.5	0.0	.879	300	4087558.	0.0000	0.00	54019	N	UN	10.0	10.0	.340	183	2632968.	0258	.83
46519	N	ST	14.0	0.0	.878	300	4071474.	0.0000	0.00	54022	N	UN	10.0	10.0	.340	183	2616265.	0511	1.65
46600	N	ST	15.0	0.0	.873	299	4089463.	0.0000	0.00	54101	N	UN	10.0	10.0	.339	183	2607326.	1021	3.30
46602	N	ST	17.0	0.0	.878	300	4078310.	0.0000	0.00	54110	N	UN	10.0	10.0	.341	184	2597940.	1526	4.95
46604	N	ST	20.0	0.0	.831	291	3955770.	0.0000	0.00	54113	N	UN	10.0	10.0	.341	184	2588267.	2030	6.60
46608	N	ST	25.0	0.0	.690	265	3626593.	0.0000	0.00	54116	N	UN	10.0	10.0	.341	184	2581336.	2535	8.25



TABLE 24.- CATALOG OF RECORDED DATA: NLR-1 AIRFOIL

A		B		A		B		A		B		A		B																
FRAME	TRIP	TYPE	AO	A1	Q	M	RE	K	FREQ	FRAME	TRIP	TYPE	AO	A1	Q	M	RE	K	FREQ	FRAME	TRIP	TYPE	AO	A1	Q	M	RE	K	FREQ	
61018	N	ST	-5.0	0.0	.122	109	1524150.	0.0000	0.00	64223	Y	ST	5.0	0.0	.339	184	2345411.	0.0000	0.00	64300	0.0000	0.00	ST	10.0	0.0	.342	185	2349991.	0.0000	0.00
61019	N	ST	0.0	0.0	.123	110	1534313.	0.0000	0.00	64301	Y	ST	10.0	0.0	.341	185	2346533.	0.0000	0.00	64304	0.0000	0.00	ST	12.0	0.0	.341	185	2346533.	0.0000	0.00
61020	N	ST	5.0	0.0	.122	110	1529480.	0.0000	0.00	64305	Y	ST	13.0	0.0	.341	185	2344262.	0.0000	0.00	64306	0.0000	0.00	ST	13.0	0.0	.341	185	2344262.	0.0000	0.00
61101	N	ST	10.0	0.0	.125	111	1537127.	0.0000	0.00	64307	Y	ST	14.0	0.0	.348	187	2370314.	0.0000	0.00	64308	0.0000	0.00	ST	14.0	0.0	.348	187	2370314.	0.0000	0.00
61102	N	ST	12.0	0.0	.122	110	1517792.	0.0000	0.00	64309	Y	ST	16.0	0.0	.344	186	2345780.	0.0000	0.00	64310	0.0000	0.00	ST	16.0	0.0	.344	186	2345780.	0.0000	0.00
61103	N	ST	14.0	0.0	.122	110	1522421.	0.0000	0.00	64311	Y	ST	0.0	0.0	.344	186	2355621.	0.0000	0.00	64312	0.0000	0.00	ST	0.0	0.0	.344	186	2355621.	0.0000	0.00
61104	N	ST	15.0	0.0	.122	110	1517668.	0.0000	0.00	65019	Y	ST	-11.0	0.0	.875	301	3814433.	0.0000	0.00				ST	-11.0	0.0	.875	301	3814433.	0.0000	0.00
61105	N	ST	14.0	0.0	.122	110	1511515.	0.0000	0.00	65020	Y	ST	-9.0	0.0	.876	301	3804399.	0.0000	0.00				ST	-9.0	0.0	.876	301	3804399.	0.0000	0.00
61106	N	ST	16.0	0.0	.121	109	1502456.	0.0000	0.00	65021	Y	ST	-7.0	0.0	.875	301	3798094.	0.0000	0.00				ST	-7.0	0.0	.875	301	3798094.	0.0000	0.00
61107	N	ST	18.0	0.0	.123	110	1511233.	0.0000	0.00	65022	Y	ST	-6.0	0.0	.874	301	3790531.	0.0000	0.00				ST	-6.0	0.0	.874	301	3790531.	0.0000	0.00
61108	N	ST	20.0	0.0	.122	110	1509433.	0.0000	0.00	65023	Y	ST	-5.0	0.0	.876	301	3792112.	0.0000	0.00				ST	-5.0	0.0	.876	301	3792112.	0.0000	0.00
61114	N	ST	0.0	0.0	.341	185	2466730.	0.0000	0.00	65100	Y	ST	0.0	0.0	.875	301	3786607.	0.0000	0.00				ST	0.0	0.0	.875	301	3786607.	0.0000	0.00
61115	N	ST	0.0	0.0	.342	185	2469459.	0.0000	0.00	65101	Y	ST	5.0	0.0	.878	302	3783080.	0.0000	0.00				ST	5.0	0.0	.878	302	3783080.	0.0000	0.00
61117	N	ST	5.0	0.0	.341	184	2461681.	0.0000	0.00	65103	Y	ST	10.0	0.0	.875	301	3764580.	0.0000	0.00				ST	10.0	0.0	.875	301	3764580.	0.0000	0.00
61201	N	ST	10.0	0.0	.341	184	2434057.	0.0000	0.00	65107	Y	ST	11.8	0.0	.842	295	3697279.	0.0000	0.00				ST	11.8	0.0	.842	295	3697279.	0.0000	0.00
61203	N	ST	12.0	0.0	.345	185	2440090.	0.0000	0.00	65109	Y	ST	13.0	0.0	.858	298	3722261.	0.0000	0.00				ST	13.0	0.0	.858	298	3722261.	0.0000	0.00
61205	N	ST	14.0	0.0	.344	186	2430259.	0.0000	0.00	65112	Y	ST	14.0	0.0	.839	294	3665290.	0.0000	0.00				ST	14.0	0.0	.839	294	3665290.	0.0000	0.00
61208	N	ST	15.4	0.0	.338	184	2407482.	0.0000	0.00	65115	Y	ST	16.0	0.0	.879	302	3745674.	0.0000	0.00				ST	16.0	0.0	.879	302	3745674.	0.0000	0.00
61212	N	ST	16.5	0.0	.342	185	2420407.	0.0000	0.00	62020	N	US	15.0	10.0	.054	073	968160.	0.985	1.30	62021	0.985	1.30	ST	16.5	0.0	.342	185	2420407.	0.0000	0.00
61213	N	ST	18.0	0.0	.341	184	2413757.	0.0000	0.00	62104	N	US	15.0	10.0	.121	109	1446202.	0.987	1.30	62105	0.987	1.30	ST	18.0	0.0	.341	184	2413757.	0.0000	0.00
61215	N	ST	20.0	0.0	.342	185	2407546.	0.0000	0.00	62112	N	US	15.0	10.0	.340	184	2513401.	1.003	3.30	62113	1.003	3.30	ST	20.0	0.0	.342	185	2407546.	0.0000	0.00
61221	N	ST	5.0	0.0	.614	250	3195467.	0.0000	0.00	62114	N	US	15.0	10.0	.396	200	2557024.	1.172	6.25	62115	1.172	6.25	ST	5.0	0.0	.614	250	3195467.	0.0000	0.00
61222	N	ST	-2.0	0.0	.612	250	3197744.	0.0000	0.00	62202	N	US	15.0	5.0	.396	200	2540409.	2.826	10.35				ST	-2.0	0.0	.612	250	3197744.	0.0000	0.00
61223	N	ST	0.0	0.0	.613	250	3194392.	0.0000	0.00	62208	N	US	15.0	10.0	.480	220	2777505.	0.974	3.93	62209	0.974	3.93	ST	0.0	0.0	.613	250	3194392.	0.0000	0.00
61300	N	ST	2.0	0.0	.612	250	3191078.	0.0000	0.00	62210	N	US	15.0	10.0	.612	250	3113246.	0.972	4.98	62211	0.972	4.98	ST	2.0	0.0	.612	250	3191078.	0.0000	0.00
61301	N	ST	2.0	0.0	.612	250	3188268.	0.0000	0.00	62218	N	US	15.0	10.0	.760	280	3441981.	0.967	4.46	62219	0.967	4.46	ST	2.0	0.0	.612	250	3188268.	0.0000	0.00
61306	N	ST	8.0	0.0	.616	251	3401485.	0.0000	0.00	62302	N	US	15.0	10.0	.838	295	3859287.	0.248	1.31	62303	0.248	1.31	ST	8.0	0.0	.616	251	3401485.	0.0000	0.00
61306	N	ST	8.0	0.0	.616	251	3401485.	0.0000	0.00	62304	N	US	15.0	10.0	.834	294	3816841.	0.496	2.62	62305	0.496	2.62	ST	8.0	0.0	.616	251	3401485.	0.0000	0.00
61306	N	ST	8.0	0.0	.616	251	3401485.	0.0000	0.00	62307	N	US	15.0	10.0	.835	294	3810660.	0.991	5.24	62308	0.991	5.24	ST	8.0	0.0	.616	251	3401485.	0.0000	0.00
61308	N	ST	10.0	0.0	.619	251	3402068.	0.0000	0.00	62309	N	US	15.0	10.0	.796	287	3699269.	1.521	7.86	62310	1.521	7.86	ST	10.0	0.0	.619	251	3402068.	0.0000	0.00
61308	N	ST	12.0	0.0	.613	249	3381325.	0.0000	0.00	62311	N	US	15.0	10.0	.872	301	3725580.	0.098	5.4	62316	0.098	5.4	ST	12.0	0.0	.613	249	3381325.	0.0000	0.00
61309	N	ST	12.5	0.0	.614	250	3381216.	0.0000	0.00	62320	N	US	10.0	10.0	.874	302	3704354.	0.243	1.34	62321	0.243	1.34	ST	12.5	0.0	.614	250	3381216.	0.0000	0.00
61310	N	ST	13.0	0.0	.610	249	3364760.	0.0000	0.00	62322	N	US	10.0	10.0	.873	301	3685360.	0.484	2.68	62323	0.484	2.68	ST	13.0	0.0	.610	249	3364760.	0.0000	0.00
61311	N	ST	14.0	0.0	.611	251	3385628.	0.0000	0.00	62400	N	US	10.0	10.0	.878	302	3685928.	0.965	5.36	62401	0.965	5.36	ST	14.0	0.0	.611	251	3385628.	0.0000	0.00
61312	N	ST	15.0	0.0	.611	249	3361196.	0.0000	0.00	62403	N	US	10.0	10.0	.881	303	3701055.	1.156	6.43	62404	1.156	6.43	ST	15.0	0.0	.611	249	3361196.	0.0000	0.00
61316	N	ST	16.0	0.0	.612	250	3357544.	0.0000	0.00	62405	N	US	10.0	10.0	.866	300	3656986.	1.457	8.04	62406	1.457	8.04	ST	16.0	0.0	.612	250	3357544.	0.0000	0.00
61317	N	ST	25.0	0.0	.612	250	3344638.	0.0000	0.00	63018	N	US	15.0	5.0	.855	297	3912793.	0.102	5.4				ST	25.0	0.0	.612	250	3344638.	0.0000	0.00
61318	N	ST	14.0	0.0	.612	250	3349019.	0.0000	0.00	63019	N	US	15.0	5.0	.862	299	3885789.	0.250	1.34				ST	14.0	0.0	.612	250	3349019.	0.0000	0.00
61400	N	ST	5.0	0.0	.614	250	3357487.	0.0000	0.00	63020	N	US	15.0	5.0	.862	299	3871332.	0.049	2.68				ST	5.0	0.0	.614	250	3357487.	0.0000	0.00
61401	N	ST	5.0	0.0	.612	249	3363498.	0.0000	0.00	63021	N	US	15.0	5.																

TABLE 24.- Concluded.

A		B								
FRAME	TRIP	TYPE	AO	A1	Q	M	RE	K	FREQ	FRAME
63320	N	US	2.5	10.0	.878	.303	3739575.	.0969	5.36	63321
63323	N	US	2.7	10.0	.880	.303	3746774.	.0969	5.36	63400
64019	Y	US	15.0	10.0	.844	.296	3865490.	.0247	1.31	64020
64021	Y	US	15.0	10.0	.840	.295	3813567.	.0493	2.62	64022
64023	Y	US	15.0	10.0	.821	.292	3752005.	.0997	5.24	64100
64107	Y	US	15.0	10.0	.340	.185	2448919.	.0496	1.65	64108
64109	Y	US	15.0	10.0	.340	.184	2439010.	.0991	3.30	64110
64111	Y	US	15.0	10.0	.341	.185	2439626.	.1481	4.95	64112
64119	Y	US	2.5	10.0	.876	.302	3823417.	.0099	1.54	64120
64121	Y	US	2.5	10.0	.875	.302	3785081.	.0244	1.34	64122
64202	Y	US	2.5	10.0	.879	.303	3794515.	.0487	2.68	64203
64204	Y	US	2.5	10.0	.878	.302	3774318.	.0974	5.36	64205
64212	Y	US	-2.0	10.0	.877	.302	3717936.	.0098	1.54	
64213	Y	US	-2.0	10.0	.878	.303	3695424.	.0241	1.34	
64214	Y	US	-2.0	10.0	.878	.302	3685179.	.0482	2.68	
64215	Y	US	-2.0	10.0	.880	.303	3683703.	.0963	5.36	
65121	N	US	-2.0	10.0	.869	.300	3717371.	.0098	1.54	
65122	N	US	-2.0	10.0	.873	.301	3700235.	.0243	1.34	
65123	N	US	-2.0	10.0	.874	.301	3694893.	.0485	2.68	
65200	N	US	-2.0	10.0	.877	.302	3694943.	.0968	5.36	
65207	N	US	15.0	10.0	.395	.199	2646668.	.0997	3.57	
65209	N	US	15.0	10.0	.828	.292	3775170.	1.019	5.36	
65223	N	US	7.0	5.0	.121	.109	1475396.	.0249	1.49	
65300	N	US	7.0	5.0	.121	.109	1472656.	.1996	3.92	
65311	N	US	7.0	5.0	.879	.301	3862901.	.1969	10.72	
65309	N	US	7.0	5.0	.876	.301	3889117.	.0100	1.54	
63222	N	US	15.0	2.0	.818	.291	3675798.	.2028	10.72	63223





TABLE 25.- Concluded.

A		B	
FRAME	TRIP	FREQ	FRAME
69100	N	1.34	69101
69102	N	2.68	69103
69105	N	5.36	69106
69107	N	8.04	69108
69119	N	1.34	69120
69121	N	2.68	69122
69123	N	5.36	69200
69201	N	10.72	69202
69206	N	1.34	69207
69208	N	2.68	69209
69211	N	5.36	69212
69213	N	8.04	69214
69215	N	10.72	69216
69221	N	2.68	69222
69223	N	5.36	69300
69304	N	10.72	69305
69310	N	2.68	69311
70019	N	5.36	70020
70021	N	8.04	70022
70023	N	10.72	70100
70107	N	1.34	70108
70109	N	2.68	70110
70113	N	5.36	70114
70115	N	10.72	70116
70117	N	1.34	70118

K	RE	H	Q	A0	A1	TYPE	AD	A1	Q	H	RE	K
.0249	3918788.	.300	.873	10.0	10.0	US	10.0	10.0	.873	.300	3918788.	.0249
.0496	3900063.	.300	.876	10.0	10.0	US	10.0	10.0	.876	.300	3900063.	.0496
.0991	3904003.	.301	.877	10.0	10.0	US	10.0	10.0	.877	.301	3904003.	.0991
.1484	3884160.	.300	.876	10.0	10.0	US	10.0	10.0	.876	.300	3884160.	.1484
.0270	3492462.	.272	.727	16.8	2.0	US	16.8	2.0	.727	.272	3492462.	.0270
.0546	3430737.	.270	.710	16.8	2.0	US	16.8	2.0	.710	.270	3430737.	.0546
.1100	3396634.	.268	.700	16.8	2.0	US	16.8	2.0	.700	.268	3396634.	.1100
.2208	3366783.	.267	.692	16.8	2.0	US	16.8	2.0	.692	.267	3366783.	.2208
.0268	3460551.	.273	.734	17.2	2.0	US	17.2	2.0	.734	.273	3460551.	.0268
.0530	3469110.	.275	.745	17.2	2.0	US	17.2	2.0	.745	.275	3469110.	.0530
.1086	3370669.	.270	.709	17.2	2.0	US	17.2	2.0	.709	.270	3370669.	.1086
.1616	3387722.	.272	.719	17.2	2.0	US	17.2	2.0	.719	.272	3387722.	.1616
.2098	3459727.	.279	.755	17.2	2.0	US	17.2	2.0	.755	.279	3459727.	.2098
.0536	3404711.	.273	.726	17.5	2.0	US	17.5	2.0	.726	.273	3404711.	.0536
.2205	3286912.	.265	.684	18.5	2.0	US	18.5	2.0	.684	.265	3286912.	.2205
.0549	3288767.	.266	.688	18.5	2.0	US	18.5	2.0	.688	.266	3288767.	.0549
.0554	3218013.	.262	.671	16.5	2.0	US	16.5	2.0	.671	.262	3218013.	.0554
.0245	2344007.	.341	.341	9.4	10.0	US	9.4	10.0	.341	.185	2344007.	.0245
.0973	2338519.	.185	.340	9.4	10.0	US	9.4	10.0	.340	.185	2338519.	.0973
.1948	2336677.	.185	.340	9.4	10.0	US	9.4	10.0	.340	.185	2336677.	.1948
.0104	3916444.	.301	.875	5.7	10.0	US	5.7	10.0	.875	.301	3916444.	.0104
.0247	3876178.	.301	.876	5.7	10.0	US	5.7	10.0	.876	.301	3876178.	.0247
.0495	3861569.	.300	.872	5.7	10.0	US	5.7	10.0	.872	.300	3861569.	.0495
.0986	3854654.	.301	.875	5.7	10.0	US	5.7	10.0	.875	.301	3854654.	.0986
.1479	3843662.	.301	.874	5.7	10.0	US	5.7	10.0	.874	.301	3843662.	.1479

ORIGINAL PAGE IS  
OF POOR QUALITY

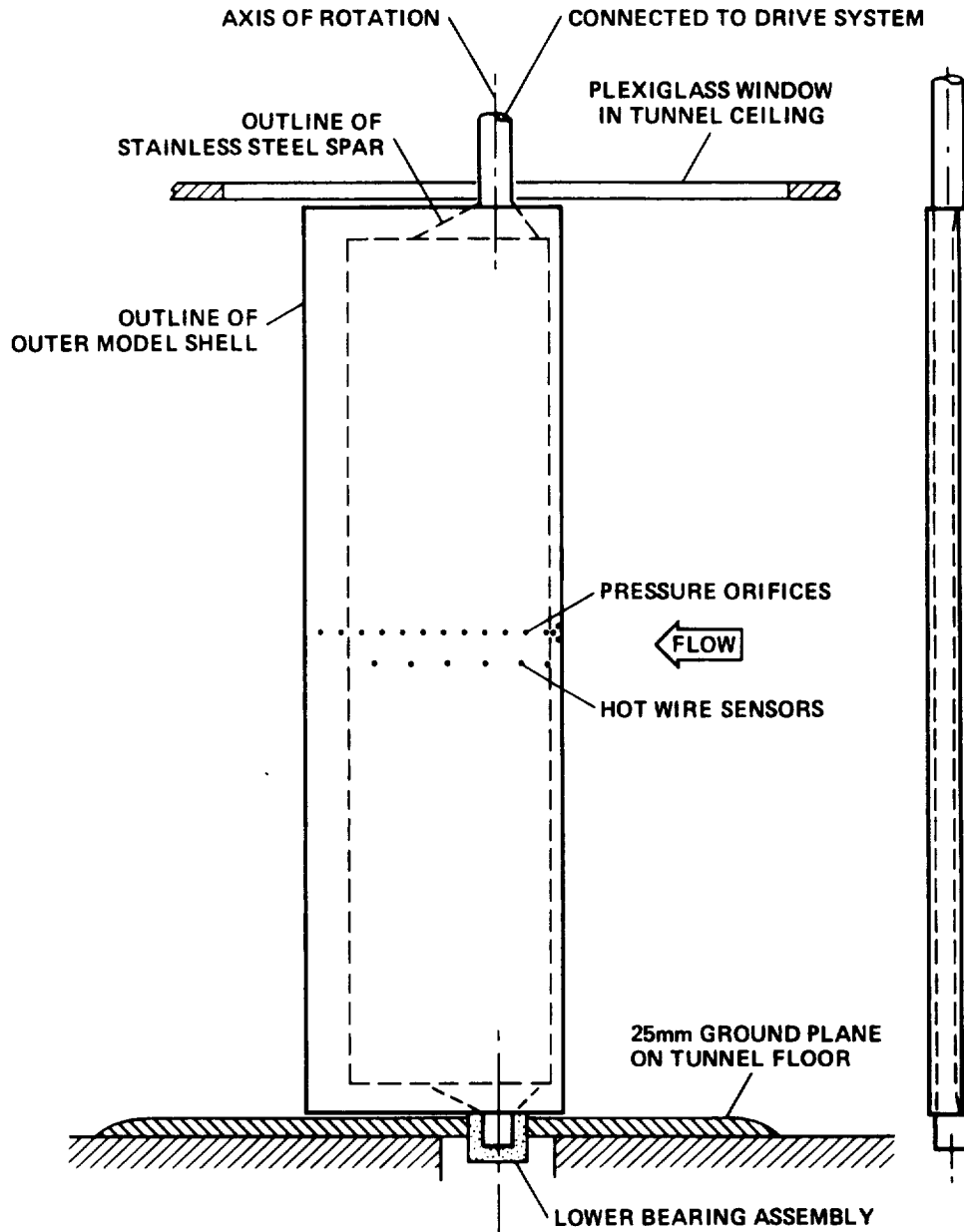
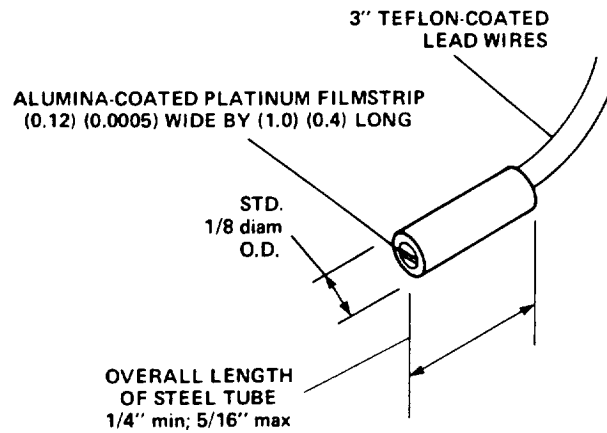


Figure 1.- Diagram showing installation of spar and airfoil shell in tunnel.

ORIGINAL PAGE IS  
OF POOR QUALITY



NOTE: PROBE MODIFIED FROM TSI MODEL 1237  
FLUSH SURFACE SENSOR

Figure 2.- Diagram of hot-film skin-friction gage.

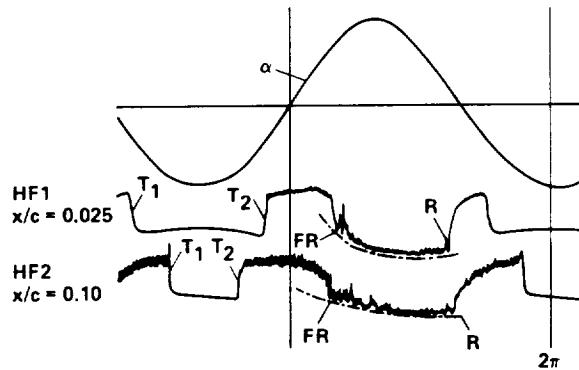


Figure 3.- Response of hot-film skin-friction gages mounted on Ames A-01  
airfoil during airfoil oscillation in pitch ( $\alpha = 15^\circ + 10^\circ \sin \omega t$ ,  
 $k = 0.10$ ,  $M_\infty = 0.22$ ).

ORIGINAL PAGE 13  
OF POOR QUALITY

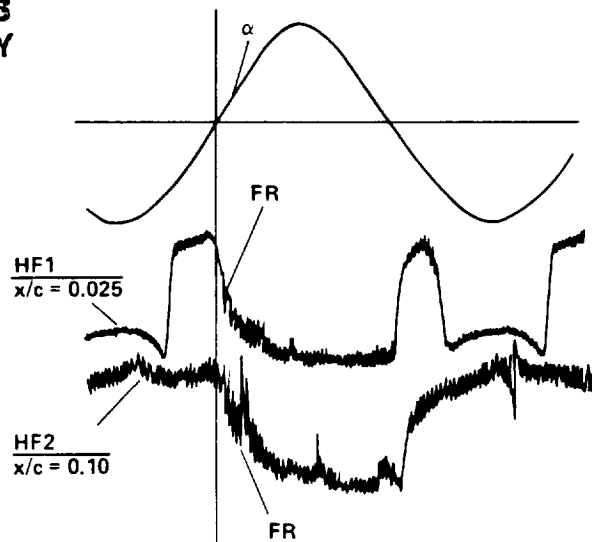


Figure 4.- Response of hot-film skin-friction gages at surface of NACA 0012 airfoil during airfoil oscillation in pitch ( $\alpha = 15^\circ + 10^\circ \sin \omega t$ ,  $k = 0.10$ ,  $M_\infty = 0.295$ ).

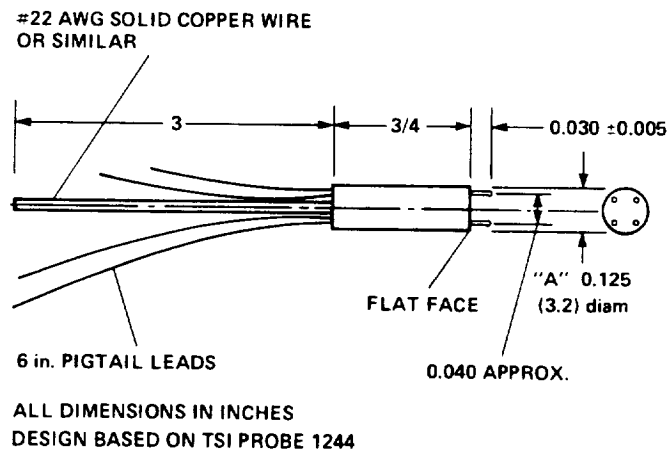


Figure 5.- Diagram of dual-element hot-wire probe.

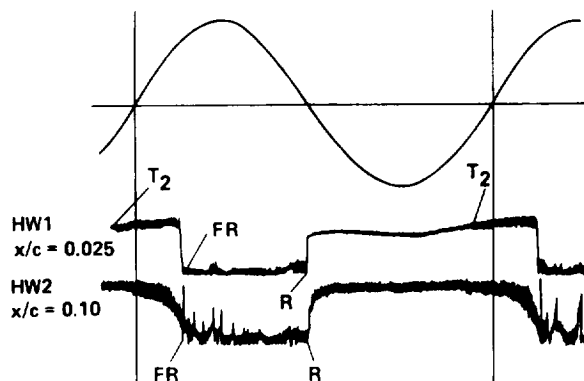


Figure 6.- Response of hot-wire anemometer probes on Wortmann FX-098 airfoil during airfoil oscillation in pitch ( $\alpha = 15^\circ + 10^\circ \sin \omega t$ ,  $k = 0.10$ ,  $M_\infty = 0.11$ ).



Figure 7.- Response of hot-wire anemometer probe installed near trailing edge of the Vertol VR-7 airfoil during oscillation in pitch.

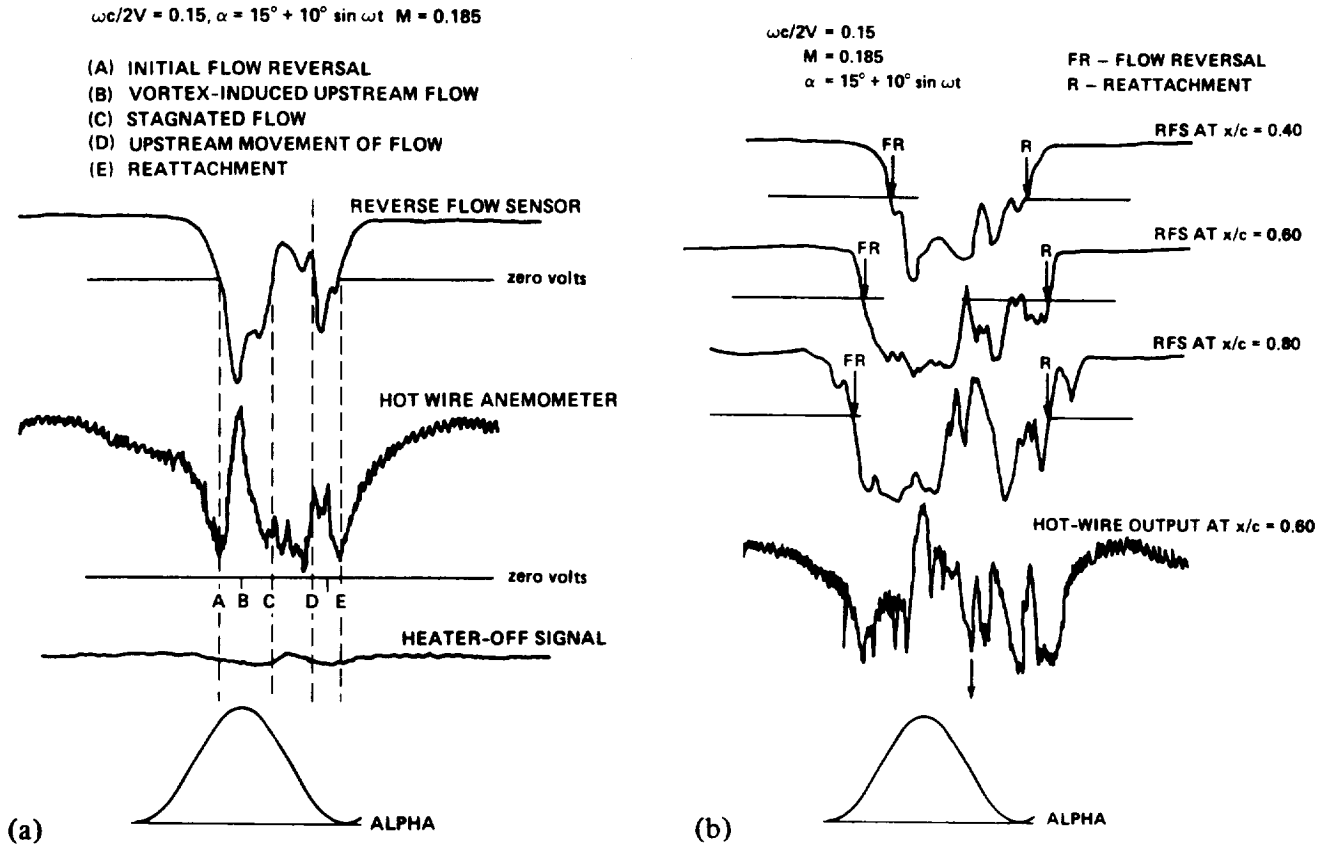
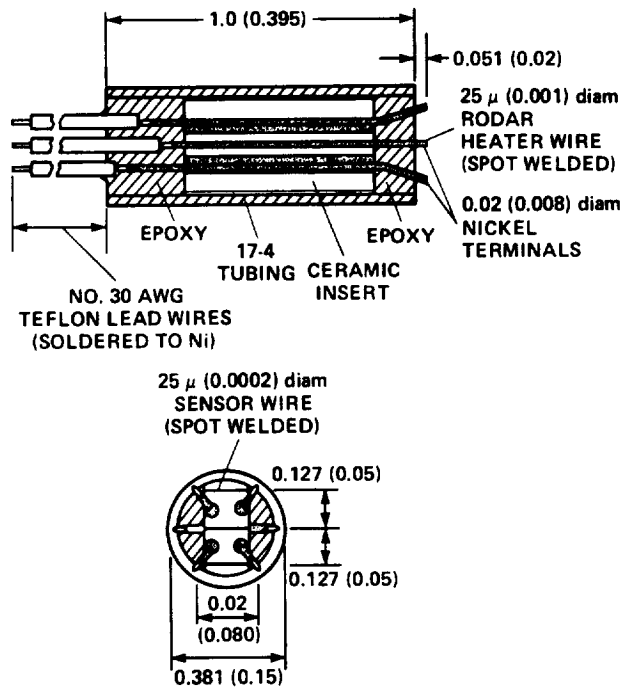


Figure 8.- Results obtained using triple-wire flow-reversal sensor:  
(a) Typical comparison of flow-reversal sensor and hot-wire anemometer  
signal (from ref. 2); (b) Progression of flow reversal up airfoil during  
dynamic stall (from ref. 2).



DIMENSIONS IN mm (ft)

Figure 9.- Diagram of three-element, directionally sensitive hot-wire probe  
(from ref. 2).

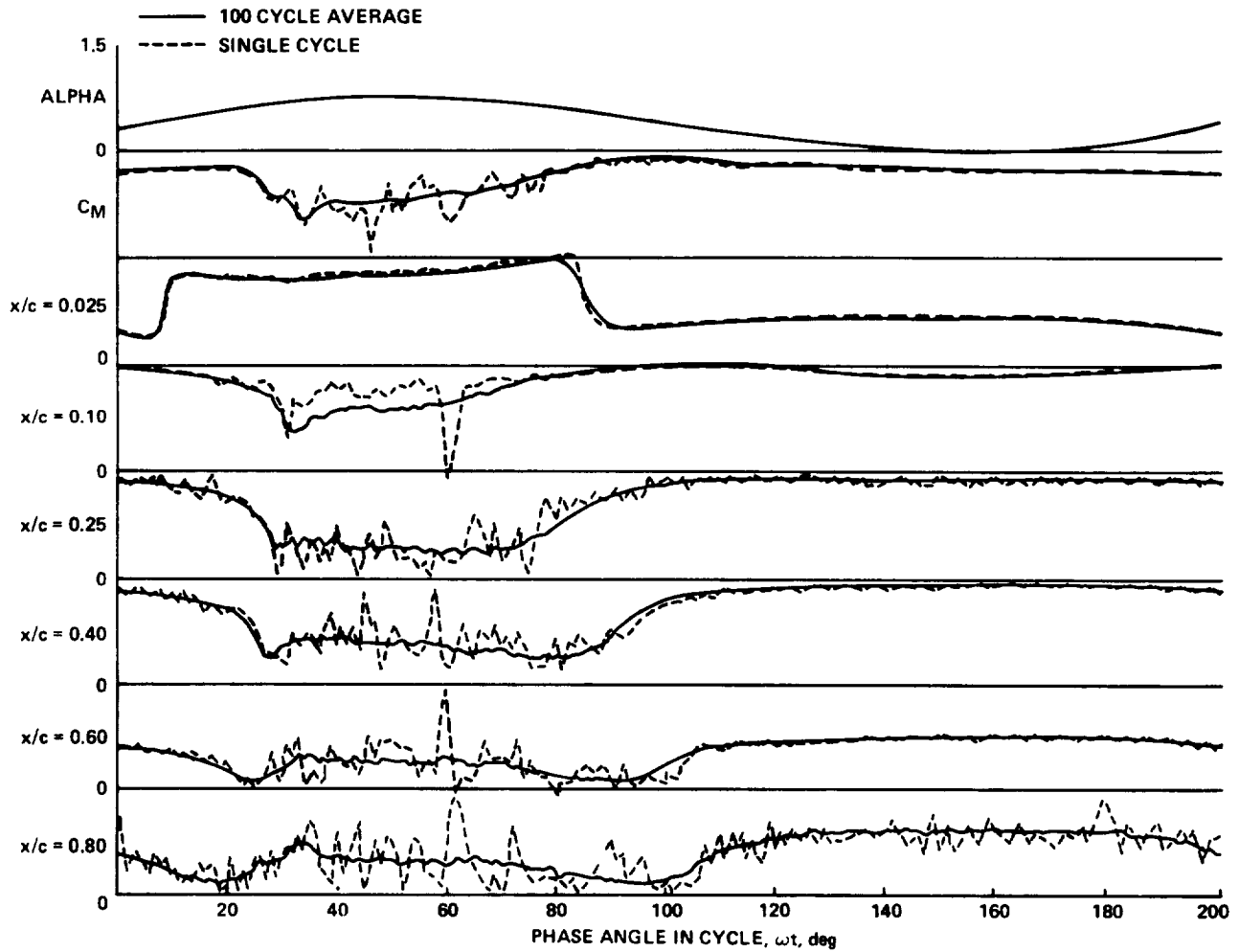


Figure 10.- Comparison of 100-cycle ensemble average and single-cycle signals from hot-wire anemometers for Vertol VR-7 airfoil during oscillation in pitch: ———, 100 cycle average; -----, single cycle.



ORIGINAL PAGE IS  
OF POOR QUALITY

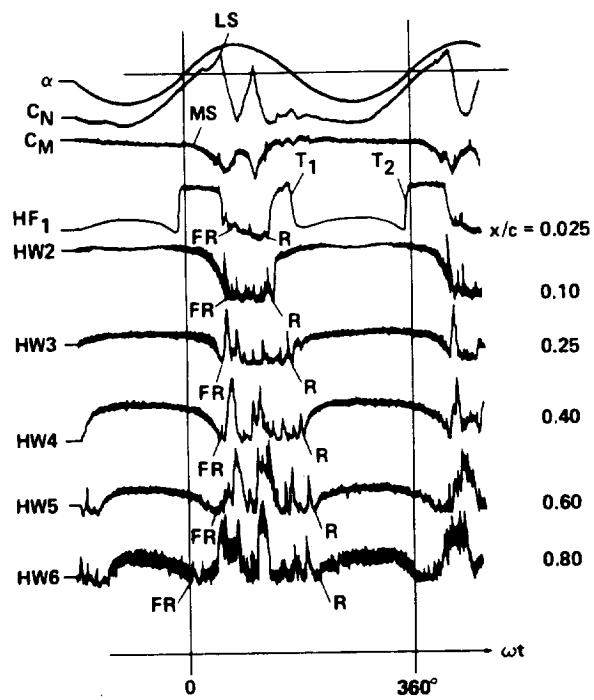


Figure 11.- Response of hot-film skin-friction gage and hot-wire anemometer probes on Vertol VR-7 during oscillation in pitch ( $\alpha = 15^\circ + 10^\circ \sin \omega t$ ,  $k = 0.10$ ,  $M_\infty = 0.185$ ).

ORIGINAL PAGE IS  
OF POOR QUALITY

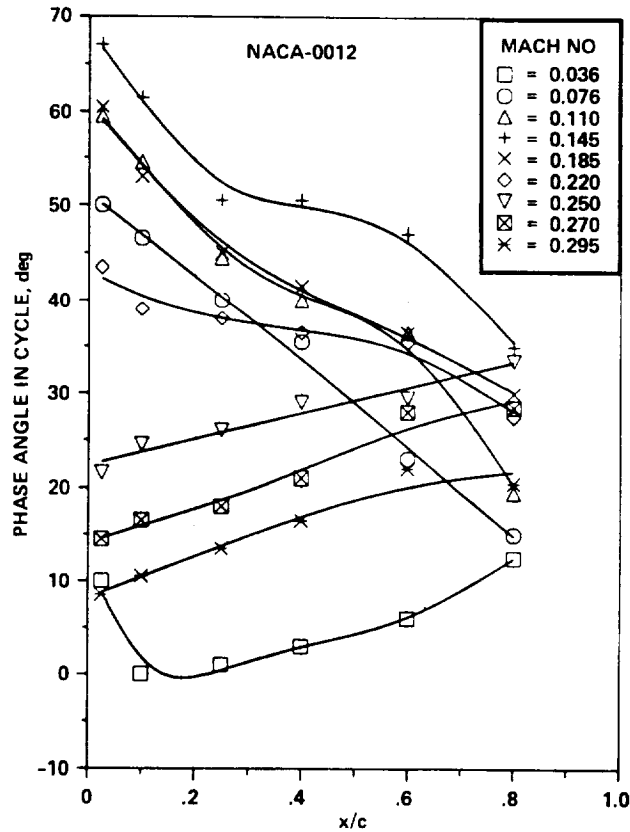


Figure 12.- Phase angle,  $\omega t$ , of flow reversal on NACA 0012 airfoil vs chord location for a range of Mach numbers at  $k = 0.1$ ,  $\alpha = 15^\circ + 10^\circ \sin \omega t$  - Mach number effects.

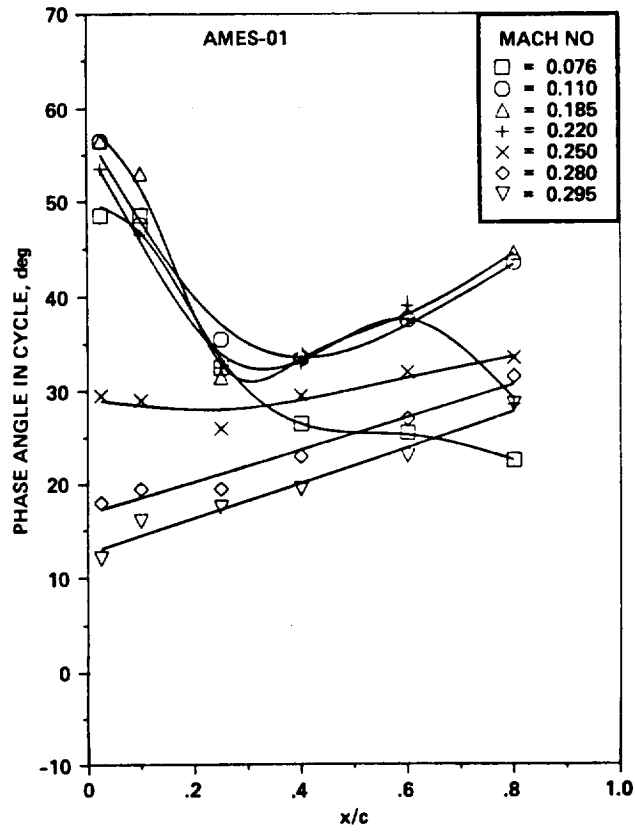


Figure 13.- Phase angle,  $\omega t$ , of flow reversal on Ames A-01 airfoil vs chord location for a range of Mach numbers at  $k = 0.1$ ,  $\alpha = 15^\circ + 10^\circ \sin \omega t$  - Mach number effects.

ORIGINAL PAGE IS  
OF POOR QUALITY

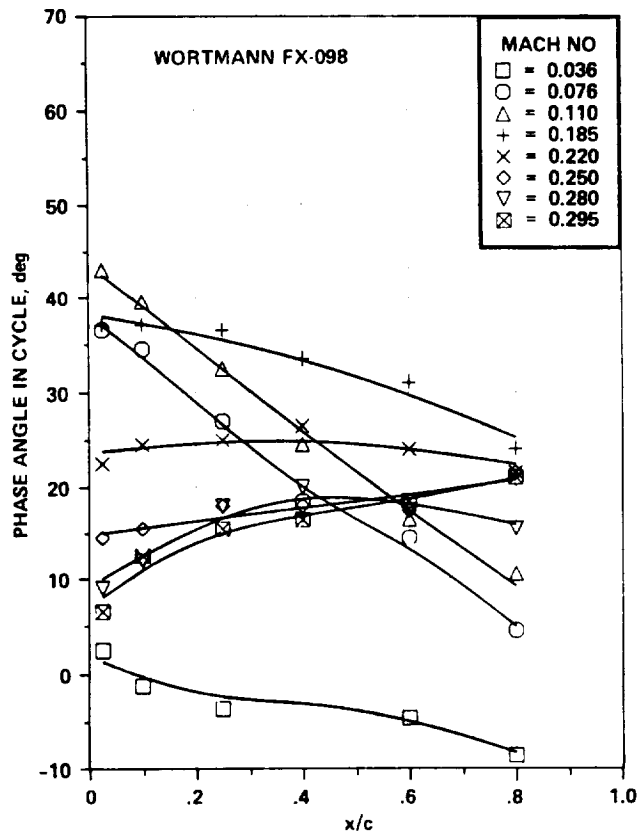


Figure 14.- Phase angle,  $\omega t$ , of flow reversal on Wortmann FX-098 airfoil vs chord location for a range of Mach numbers at  $k = 0.1$ ,  $\alpha = 15^\circ + 10^\circ \sin \omega t$  - Mach number effects.

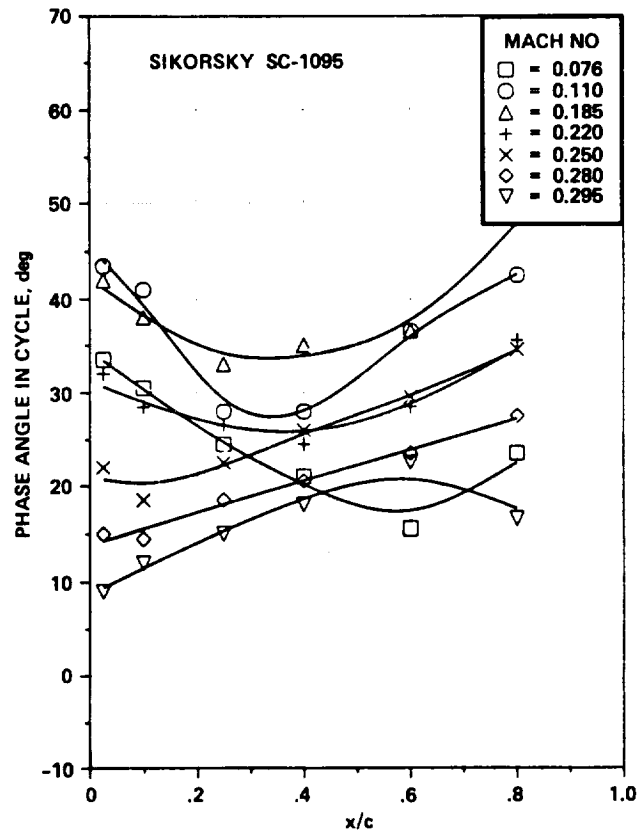


Figure 15.- Phase angle,  $\omega t$ , of flow reversal on Sikorsky SC-1095 airfoil vs chord location for a range of Mach numbers at  $k = 0.1$ ,  $\alpha = 15^\circ + 10^\circ \sin \omega t$  - Mach number effects.

ORIGINAL PAGE IS  
OF POOR QUALITY

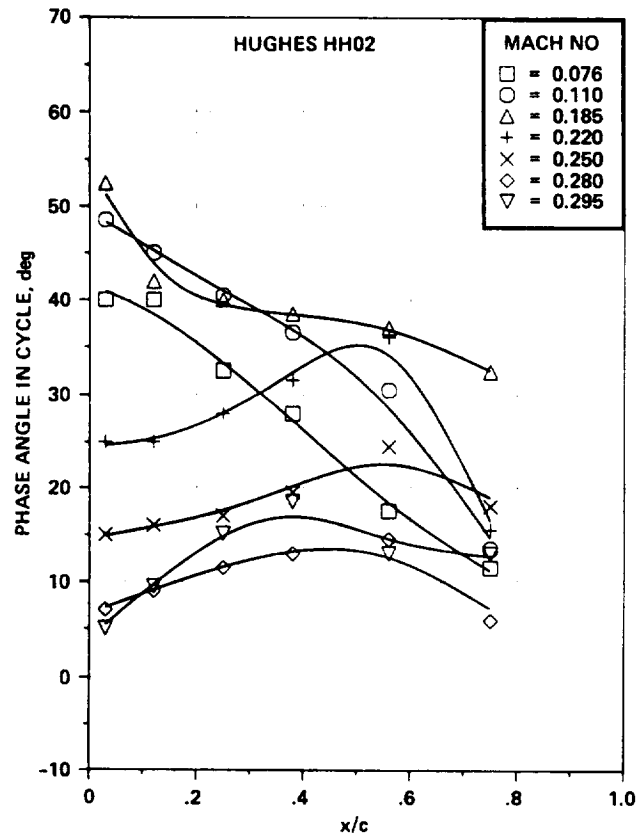


Figure 16.- Phase angle,  $\omega t$ , of flow reversal on Hughes HH-02 airfoil vs chord location for a range of Mach numbers at  $k = 0.1$ ,  $\alpha = 15^\circ + 10^\circ \sin \omega t$  - Mach number effects.

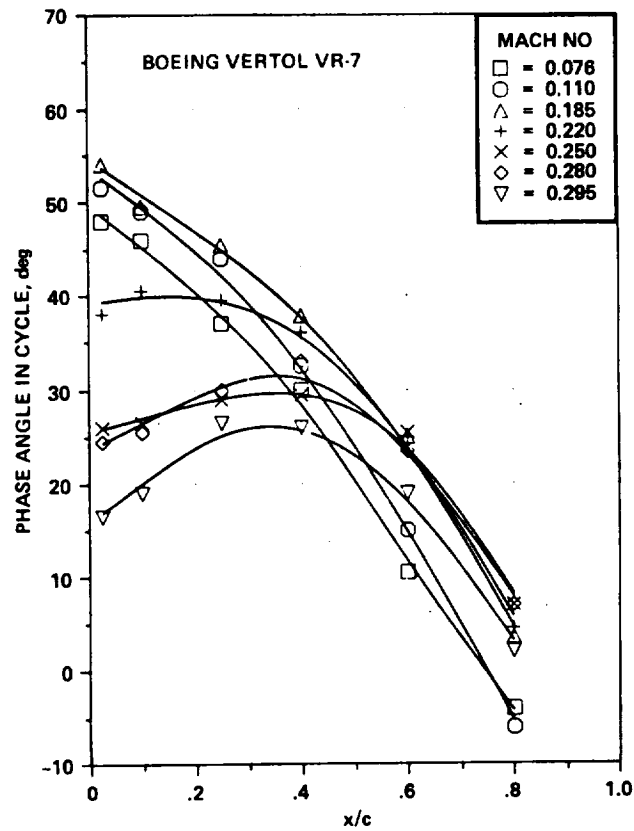


Figure 17.- Phase angle,  $\omega t$ , of flow reversal on Vertol VR-7 airfoil vs chord location for a range of Mach numbers at  $k = 0.1$ ,  $\alpha = 15^\circ + 10^\circ \sin \omega t$  - Mach number effects.

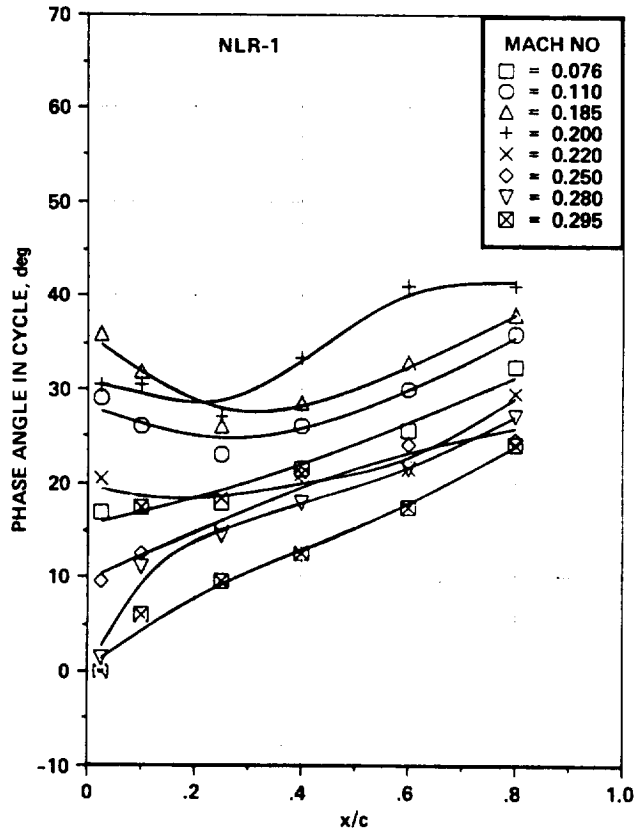


Figure 18.- Phase angle,  $\omega t$ , of flow reversal on NLR-1 airfoil vs chord location for a range of Mach numbers at  $k = 0.1$ ,  $\alpha = 15^\circ + 10^\circ \sin \omega t$  - Mach number effects.



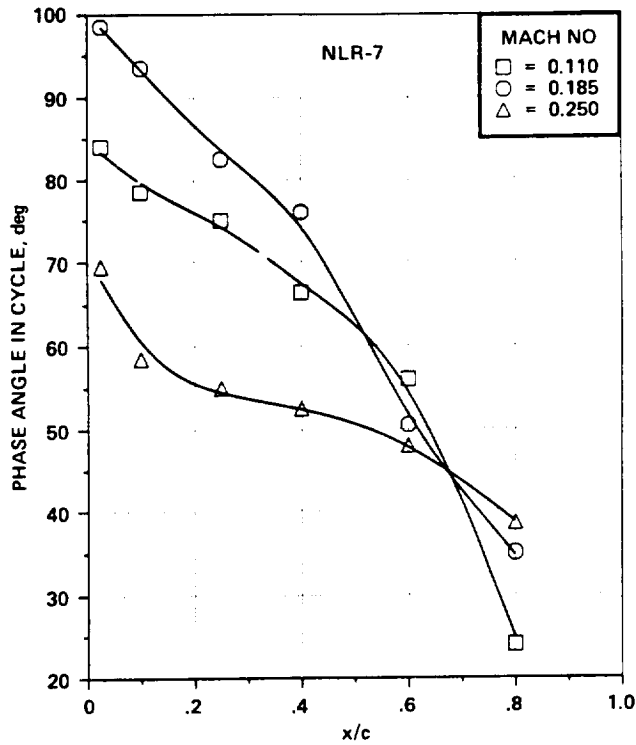


Figure 19.- Phase angle,  $\omega t$ , of flow reversal on NLR-7 airfoil vs chord location for a range of Mach numbers at  $k = 0.1$ ,  $\alpha = 15^\circ + 10^\circ \sin \omega t$  - Mach number effects.

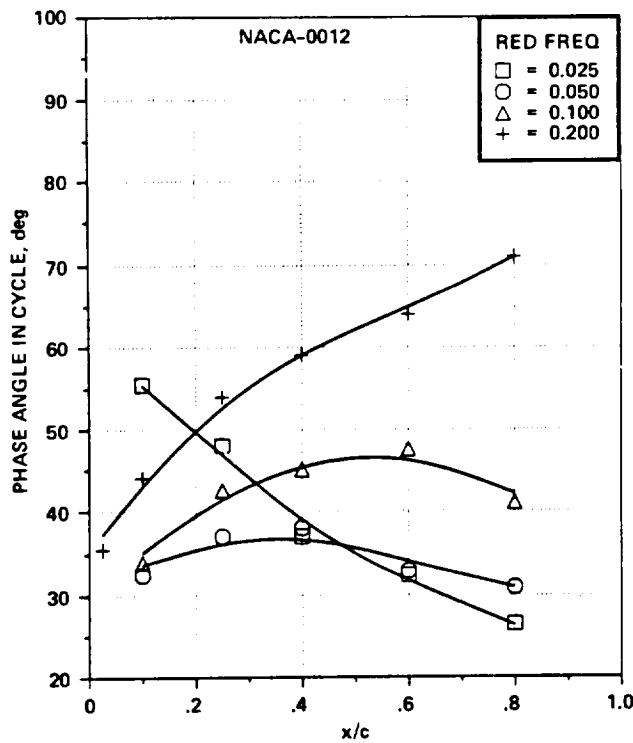


Figure 20.- Phase angle,  $\omega t$ , of flow reversal on NACA 0012 airfoil vs chord location for a range of frequencies at  $M_\infty = 0.295$ ,  $\alpha = 12^\circ + 5^\circ \sin \omega t$  - light-stall conditions.

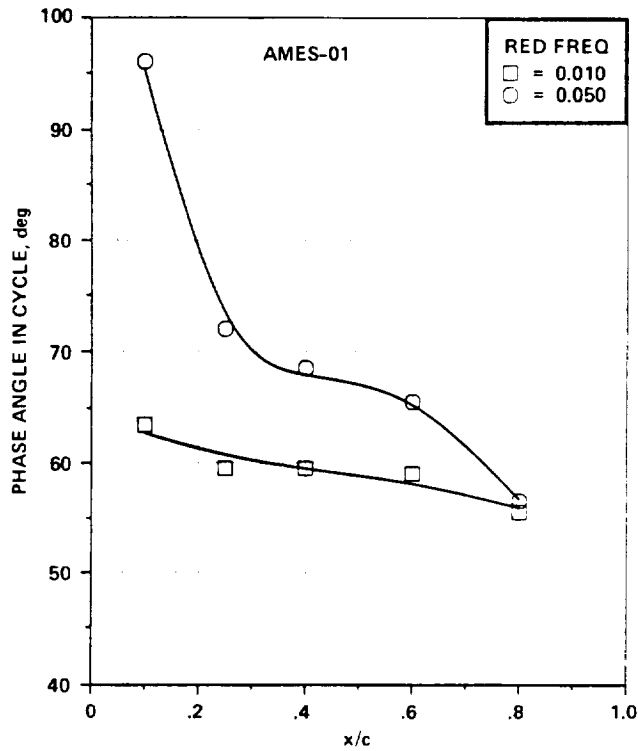


Figure 21.- Phase angle,  $\omega t$ , of flow reversal on Ames A-01 airfoil vs chord location for a range of frequencies at  $M_\infty = 0.295$ ,  $\alpha = 11^\circ + 5^\circ \sin \omega t$  - light-stall conditions.

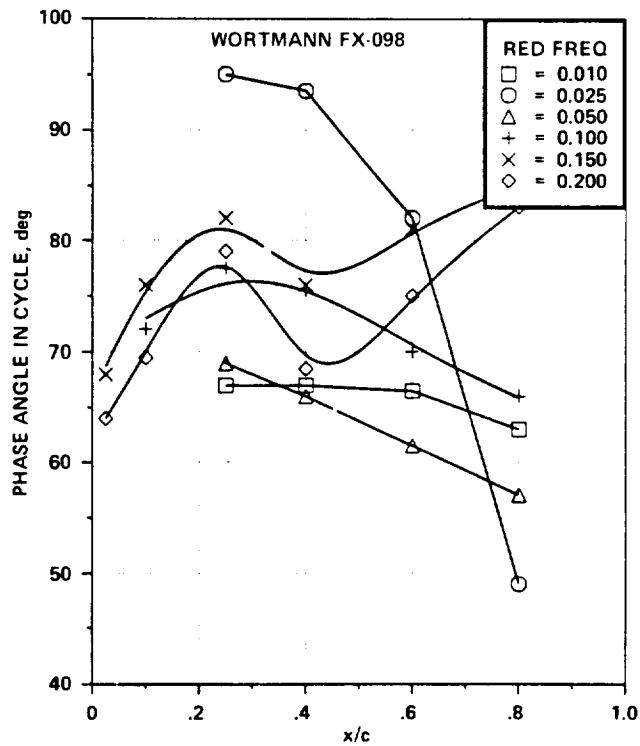


Figure 22.- Phase angle,  $\omega t$ , of flow reversal on Wortmann FX-098 airfoil vs chord location for a range of frequencies at  $M_\infty = 0.295$ ,  $\alpha = 10^\circ + 5^\circ \sin \omega t$  - light-stall conditions.

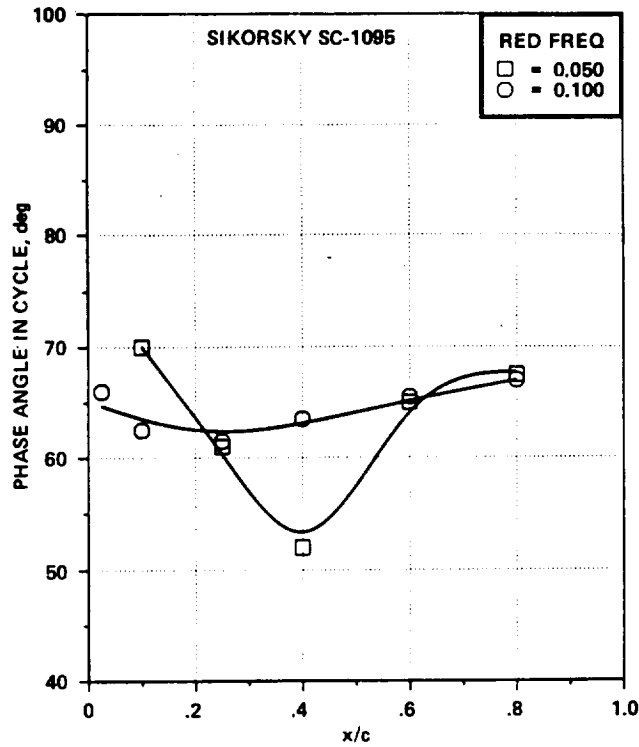


Figure 23.- Phase angle,  $\omega t$ , of flow reversal on Sikorsky SC-1095 airfoil vs chord location for a range of frequencies at  $M_\infty = 0.295$ ,  $\alpha = 11^\circ + 5^\circ \sin \omega t$  - light-stall conditions.

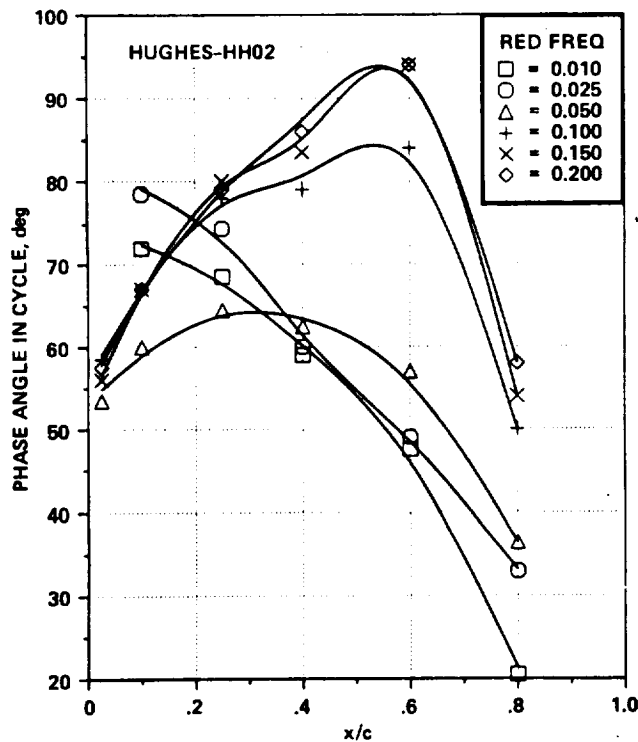


Figure 24.- Phase angle,  $\omega t$ , of flow reversal on Hughes HH-02 airfoil vs chord location for a range of frequencies at  $M_\infty = 0.295$ ,  $\alpha = 10^\circ + 5^\circ \sin \omega t$  - light-stall conditions.

ORIGINAL PAGE IS  
OF POOR QUALITY

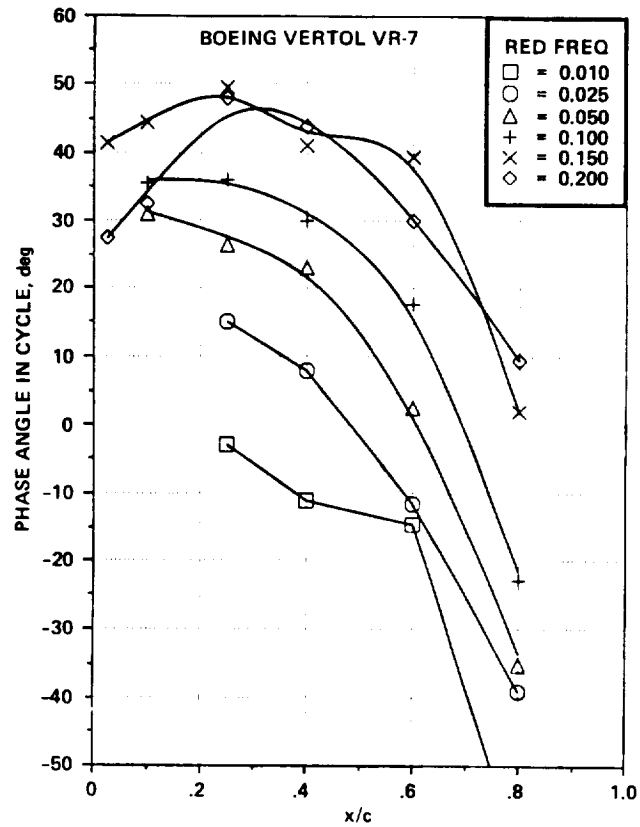


Figure 25.- Phase angle,  $\omega t$ , of flow reversal on Vertol VR-7 airfoil vs chord location for a range of frequencies at  $M_\infty = 0.295$ ,  $\alpha = 15^\circ + 5^\circ \sin \omega t$  - light-stall conditions.

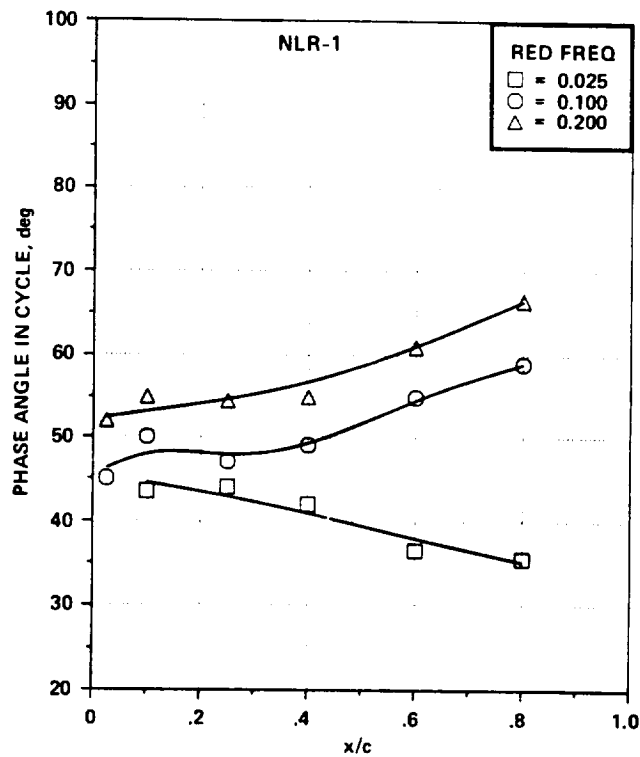


Figure 26.- Phase angle,  $\omega t$ , of flow reversal on NLR-1 airfoil vs chord location for a range of frequencies at  $M_\infty = 0.295$ ,  $\alpha = 10^\circ + 5^\circ \sin \omega t$  - light-stall conditions.

ORIGINAL PAGE IS  
OF POOR QUALITY

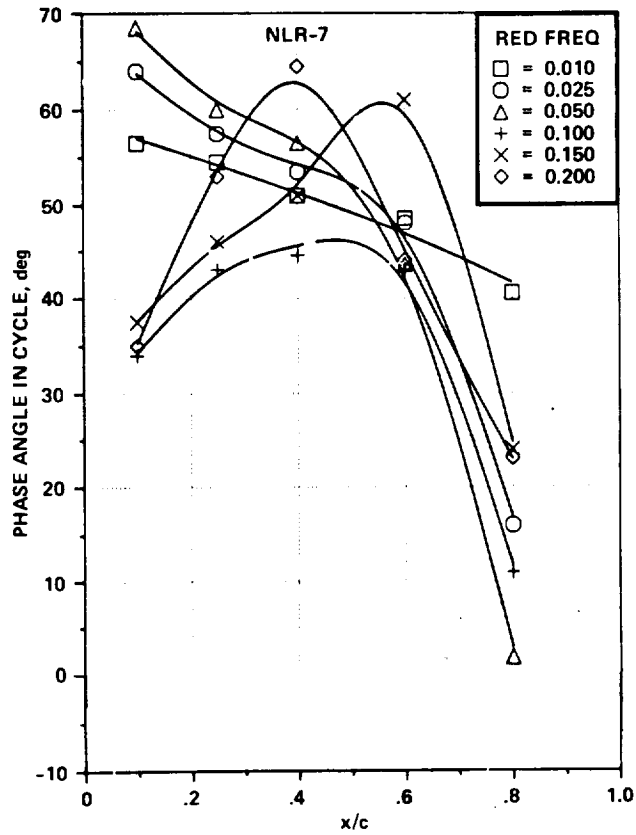


Figure 27.- Phase angle,  $\omega t$ , of flow reversal on NLR-7 airfoil vs chord location for a range of frequencies at  $M_\infty = 0.295$ ,  $\alpha = 15^\circ + 5^\circ \sin \omega t$  - light-stall conditions.

ORIGINAL PAGE IS  
OF POOR QUALITY

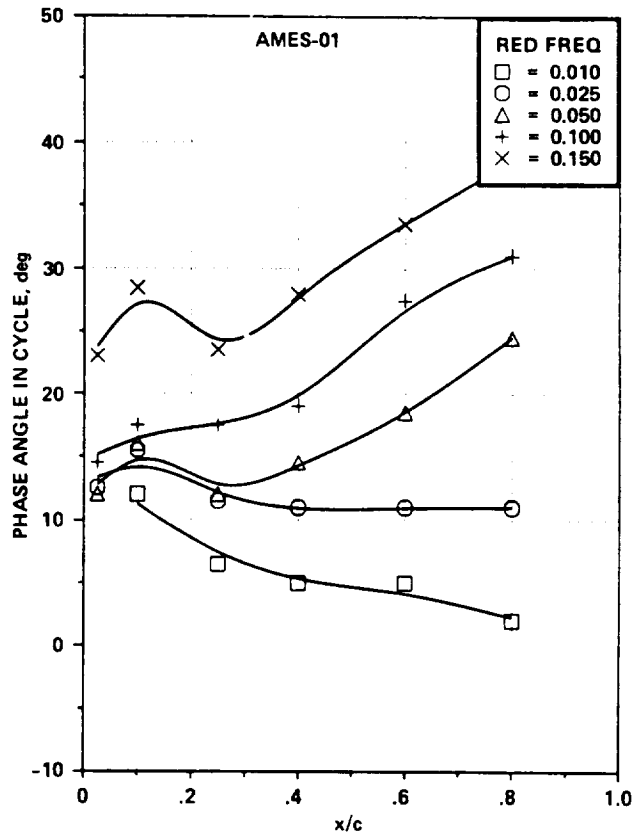


Figure 28.- Phase angle,  $\omega t$ , of flow reversal on Ames A-01 airfoil vs chord for a range of frequencies at  $M_\infty = 0.295$ ,  $\alpha = 15^\circ + 10^\circ \sin \omega t$  - deep-stall conditions.

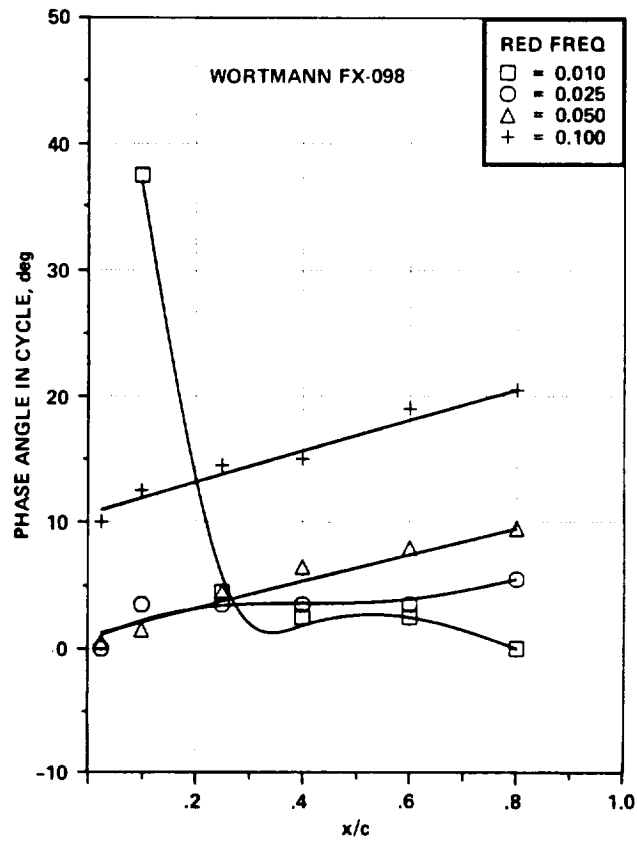


Figure 29.- Phase angle,  $\omega t$ , of flow reversal on Wortmann W-98 airfoil vs chord for a range of frequencies at  $M_\infty = 0.295$ ,  $\alpha = 15^\circ + 10^\circ \sin \omega t$  - deep-stall conditions.

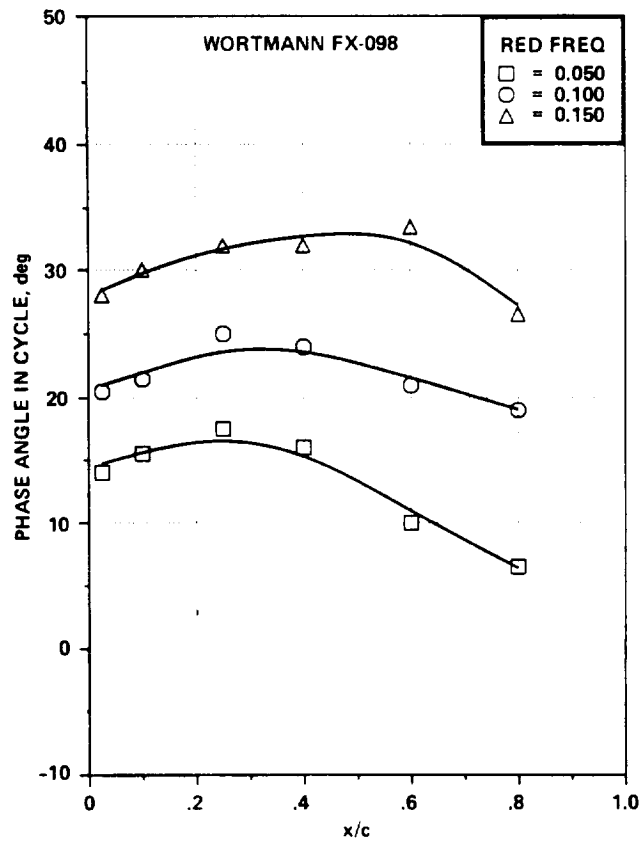


Figure 30.- Phase angle,  $\omega t$ , of flow reversal on Wortmann FX-098 airfoil vs chord for a range of frequencies at  $M_\infty = 0.185$ ,  $\alpha = 15^\circ + 10^\circ \sin \omega t$  - deep-stall conditions.



ORIGINAL PAGE IS  
OF POOR QUALITY

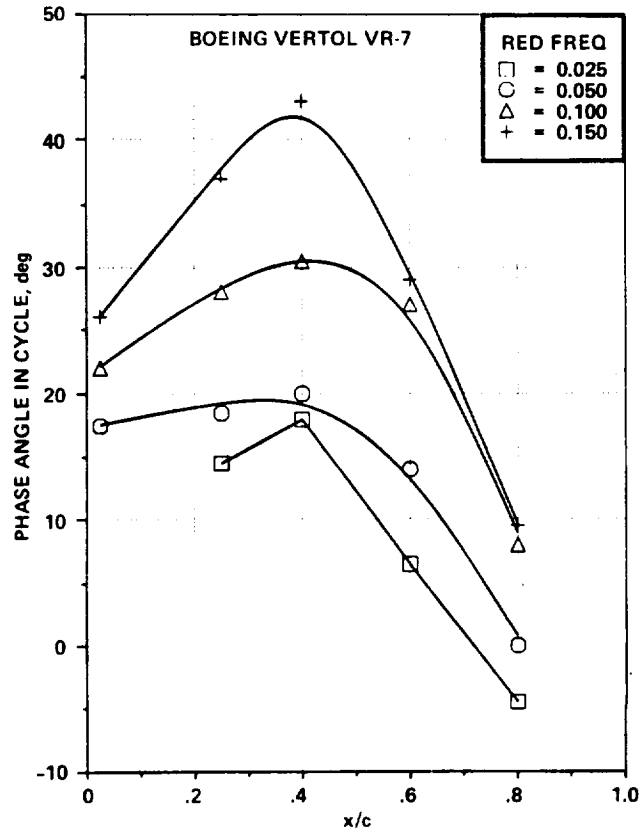


Figure 31.- Phase angle,  $\omega t$ , of flow reversal on Vertol VR-7 airfoil vs chord for a range of frequencies at  $M_\infty = 0.295$ ,  $\alpha = 15^\circ + 10^\circ \sin \omega t$  - deep-stall conditions.

1. Report No. NASA TM-84245 USAAVRADCOM TR-82-A-8		2. Government Accession No.		3. Recipient's Catalog No.	
4. Title and Subtitle AN EXPERIMENTAL STUDY OF DYNAMIC STALL ON ADVANCED AIRFOIL SECTIONS VOLUME 3. HOT-WIRE AND HOT-FILM MEASUREMENTS				5. Report Date December 1982	
				6. Performing Organization Code	
7. Author(s) L. W. Carr, W. J. McCroskey, K. W. McAlister, S. L. Pucci, and O. Lambert*				8. Performing Organization Report No. A-8938	
9. Performing Organization Name and Address NASA Ames Research Center, Moffett Field, Calif. 94035, and U.S. Army Aero- mechanics Laboratory (AVRADCOM), Ames Research Center, Moffett Field, Calif. 94035				10. Work Unit No. K-1585	
				11. Contract or Grant No.	
12. Sponsoring Agency Name and Address National Aeronautics and Space Administration, Washington, D.C. 20546, and U.S. Army Aviation R&D Command, St. Louis, MO 93166				13. Type of Report and Period Covered Technical Memorandum	
				14. Sponsoring Agency Code	
15. Supplementary Notes *Service Technique des Constructions Aéronautiques, Paris, France. Point of Contact: L. W. Carr, Ames Research Center, MS 215-1, Moffett Field, Calif. 94035. (415) 965-5892 or FTS 448-5892.					
16. Abstract  Detailed unsteady boundary-layer measurements are presented for eight airfoils oscillated in pitch through the dynamic-stall regime. The present report (the third of three volumes) describes the techniques developed for analysis and evaluation of the hot-film and hot-wire signals, offers some interpretation of the results, and tabulates all the cases in which flow reversal has been recorded.					
17. Key Words (Suggested by Author(s)) Dynamic stall                      Maximum lift Oscillating airfoils              Airfoil data Boundary layer measurements Unsteady pressure distributions			18. Distribution Statement  Unlimited  Subject Category - 02		
19. Security Classif. (of this report) Unclassified		20. Security Classif. (of this page) Unclassified		21. No. of Pages 67	22. Price* A04